UNIVERSITY OF ICELAND

M.S. Thesis

in Industrial Biotechnology

Development of mAb production batch fingerprint based on in-line capacitance measurements

Sigrún Rósa Hrólfsdóttir

June 2023

FACULTY OF PHYSICAL SCIENCES

Development of mAb production batch fingerprint based on in-line capacitance measurements

Sigrún Rósa Hrólfsdóttir

60 ECTS thesis submitted in partial fulfillment of a
Magister Scientiarum degree in Industrial Biotechnology

Supervisory teacher
Jens Guðmundur Hjörleifsson

Advisor
Adrianna Milewska

Faculty of Physical Sciences
School of Engineering and Natural Sciences
University of Iceland
Reykjavik, June 2023

Development of mAb production batch fingerprint based on in-line capacitance measurements
Dissertation submitted in partial fulfillment of an *M.S.* degree in Industrial Biotechnology

Faculty of Physical Sciences
School of Engineering and Natural Sciences
University of Iceland
Dunhagi 5
107, Reykjavik
Iceland

Telephone: 525 4000

Abstract

Viable cell density (VCD) is a highly important parameter in mammalian cell cultivations, typically measured offline. In accordance with the process analytical technology (PAT) initiative, which aims to allow for better process understanding and control, there has been a focus on the development of analytical technology allowing real-time monitoring of important culture parameters. Dielectric spectroscopy, or capacitance technology, has gained popularity for in-line monitoring of VCD. This method is based on applying electric fields to the suspension, resulting in live cells becoming polarized. Live cells contribute to the readings, while dead cells and other particles show less of a signal. Here, capacitance probes were included in two different CHO cell processes producing mAb target products in scales ranging from 15 L to 250 L. Batch fingerprints for both processes were developed, which may serve as golden batch trajectories to which future batches are compared. Biomass factor optimization was done for each proces, resulting in a general biomass factor that can be used to convert capacitance readings into VCD measurements in real-time, allowing continuous monitoring of VCD and quick detection of process deviations. Comparisons of capacitance trends across different scales revealed no systematic differences between scales, indicating that the processes were robust and scalable, and that capacitance can be used to reliably monitor VCD during process scale-up. Consistent with the literature, the single-frequency capacitance measurements used here provided highly accurate VCD predictions during the exponential growth phase, but lost accuracy in later stages of the cultivation. Thus, there is an opportunity for further improvement in in-line VCD measurements for these processes, as well as any future processes, which may be achieved using multi-frequency capacitance measurements.

Útdráttur

Frumuþéttleiki (e. viable cell density) er einn af lykilþáttum sem þarf að mæla í frumurækt. Frumuþéttleiki er yfirleitt mældur með því að taka sýni úr frumuræktinni og mæla í frumuteljara. Á síðustu árum hefur mikil áhersla verið lögð á þróun aðferða sem nota má til að fylgjast með mikilvægum þáttum í frumurækt í rauntíma, þ.e.a.s. án þess að þurfa að fjarlægja sýni í hvert skipti sem mælingar eru gerðar. Ein slík aðferð er notkun himnurýmdarmæla (e. capacitance probes), sem búa til rafsvið í lausninni sem verður til þess að frumur með heila frumuhimnu (lifandi frumur) skautast. Dauðar frumur og önnur efni í lausninni skautast síður og hafa því lítil áhrif á mælingarnar. Í þessu verkefni voru himnurýmdarmælar notaðir í tveimur mismunandi líftæknilyfja framleiðsluferlum sem notast við CHO frumur, á mismunandi skölum frá 15 L upp í 250 L. Staðalhimnurýmdarferlar (e. batch fingerprints), þ.e.a.s. himnurýmdarferlar við hefðbundnar aðstæður, voru búnir til fyrir báða ferlana, en þá má nota sem viðmið í hvert sinn sem framleiðsluferlið er endurtekið. Lífmassa-stuðlar (e. biomass factors), sem notaðir eru til að breyta himnurýmdarmælingum í frumuþéttleika, voru þróaðir fyrir báða ferlana. Með því að fylgjast með frumuþéttleika í rauntíma er hægt að taka eftir frávikum frá staðalhimnurýmdarferlinum um leið og þau eiga sér stað og bregðast við þeim fyrr. Samanburður á himnurýmdarferlum sýndi engan áberandi mun á milli skala, sem gefur í skyn að þessir ferlar séu skalanlegir og að himnurýmdarmælingar nýtast í frumuþéttleikamælingar við ferlastækkun (e. process scale-up). Eins og búist var við samkvæmt fyrri rannsóknum gátu himnurýmdarmælingarnar spáð fyrir um frumuþéttleika með mikilli nákvæmni í vaxtarfasa (e. exponential growth phase), en ekki í stöðufasa og dauðafasa. Hér voru einungis notuð gögn frá einni bylgjulengd, en með því að nota mælingar frá mörgum mismunandi bylgjulengdum er í framtíðinni hægt að þróa enn nákvæmari rauntímamælingar á frumuþéttleika í þessum ferlum.

Table of contents

List of Figures

List of Tables

Abbreviations

ADCC	Antibody-dependent cellular cytotoxicity
ADCP	Antibody-dependent cellular phagocytosis
BHK	Baby hamster kidney cells
CDCC	Complement-dependent cellular cytotoxicity
CHO	Chinese hamster ovary cells
DO	Dissolved oxygen
FDA	Food and Drug Administration
EMA	European Medicines Agency
f_C	Characteristic frequency
FTIR	Fourier-transform infrared
IPA	Isopropyl alcohol
mAb	Monoclonal antibody
NIR	Near-infrared
NK cells	Natural killer cells
PAT	Process analytical technology
pF	Pico-Farad
PLS	Partial least squares
PTM	Post-translational modifications
Q_p	Specific productivity
SUB	Single use bioreactor
TNF- α	Tumor necrosis factor-α
VCD	Viable cell density
VCV	Viable cell volume

Acknowledgements

I would like to thank my advisor, Adrianna Milewska, for supporting me and providing me with the guidance I needed to complete this project. To my supervisory teacher, Jens Guðmundur Hjörleifsson, thank you for your support throughout my Masters' studies. Finally, I would like to express my gratitude to Alvotech for the opportunity to carry out this project in their facility and providing me with the resources I needed, and to the Pilot Team for helping me learn the skills needed to carry out the experiments.

1 Introduction

1.1 Biopharmaceuticals and biosimilars

Biopharmaceuticals, or biologics, are pharmaceutical products that are produced using living cells or organisms. Compared to traditional small-molecule drugs, these molecules are much larger and more complex in structure (Makurvet, 2021). A biosimilar is a biologic that has been developed to be highly similar to another biologic medicine (the reference product) which has already been approved for use (Ishii-Watabe & Kuwabara, 2019).

In recent years, the market for biologics has grown significantly, and is expected to continue growing. As the patents of many of these biologics are starting to expire, biosimilar developers are presented with new opportunities for biosimilar development. By introducing biosimilars to the market, the reference product no longer has a market monopoly, allowing supply of the drug at lower prices for consumers (Moorkens et al., 2016).

Once a new biologic is approved, it has data and market exclusivity for 4 years and 12 years, respectively. Once the data exclusivity of the reference product expires, other companies may begin development of a biosimilar. However, the product may not enter the market until the market exclusivity of the reference product has expired (Heled, 2012). The process of biosimilar development is generally longer and significantly more expensive than that of generics (a generic's reference product is a small-molecule drug) (Blackstone & Joseph, 2013).

One of the difficulties in the development of biopharmaceuticals comes from their inherent variability (Vulto & Jaquez, 2017). Due to this variability, extensive analytical testing has to be performed on the product to ensure its biosimilarity to the reference product. Some properties of the biosimilar are required to be identical to the reference product, including the amino acid sequence, posology and route of administration (European Medicines Agency [EMA], 2014). However, there are some aspects that may differ if properly justified, including the excipients used in the final formulation. By proving that the biosimilar has the

same quality, safety and efficacy properties as the reference product using comparative analytical studies (clinical and non-clinical), the new product does not need to complete the same extensive clinical trials as the reference product (EMA, 2019).

1.2 mAbs

Many of the currently approved biosimilars are monoclonal antibodies (mAbs), which are complex glycoproteins that are able to specifically bind to a target due to the sequences in their variable regions (Chiu et al., 2019; European Medicines Agency, 2022c).

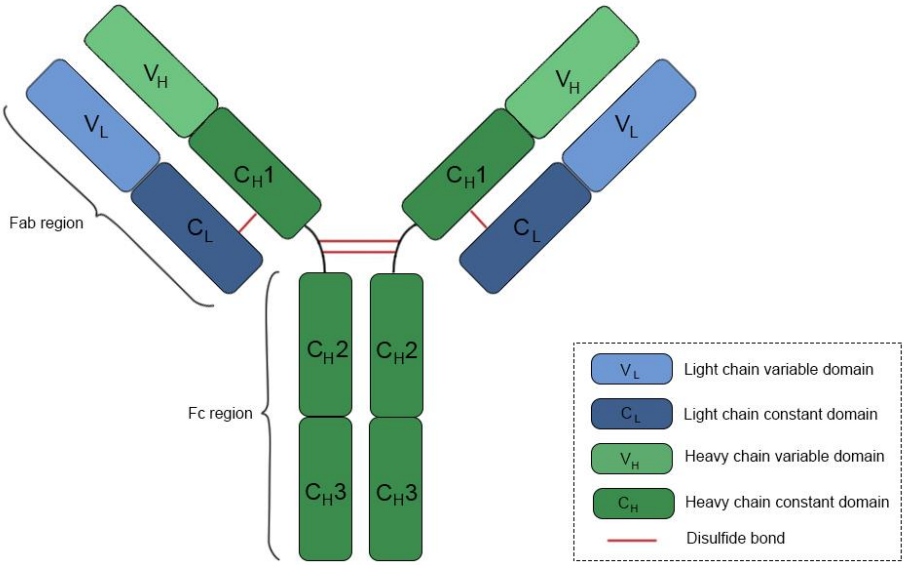

Figure 1.1 – General structure of an IgG1 antibody.

The typical structure of an IgG antibody is shown in Figure 1.1. mAbs are Y-shaped, and consist of two heavy chains and two light chains. The variable regions are located at the end of each chain in the Fab region. The other end of the antibody is called the Fc region (Nezlin, 1998). Many cells of the immune system have receptors that recognize the Fc region (Fc receptors, FcRs) (Zahavi & Weiner, 2020). This allows cells such as natural killer cells (NK cells) and other effector cells to "attack" the targeted cell through cellular processes like antibody-dependent cellular cytotoxicity (ADCC) or complement-dependent cellular cytotoxicity (CDCC) after the antibody has bound to its target (Zahavi & Weiner, 2020).

These molecules are currently used to treat a variety of diseases, including various cancers and autoimmune disorders (Lu et al., 2020). Cancer cells often overexpress certain receptors on their surfaces. By designing mAbs to specifically bind to those receptors, immune cells can be directed towards cancer cells (Shuptrine et al., 2012). Another approach is to use mAbs to target proteins that cells interact with, i.e. antigen clearance. An example of such an interaction is infliximab, which is used to treat various autoimmune diseases. Infliximab binds to tumor necrosis factor-α (TNF-α), a cytokine that is involved in the development of these diseases, thus preventing it from binding to receptors on cells (Keating & Perry, 2002).

The first biosimilar product approved in the EU was Omnitrope, a biosimilar of somatropin (the reference product was developed by Genotropin®), a recombinant human growth hormone (Schiestl et al., 2017). The first biosimilar mAbs were approved a few years later in 2013, when the infliximab biosimilars Inflectra and Remsima (developed by Hospira® and Celltrion®, respectively), were approved by the European Medicines Agency (EMA) (EMA, 2022a, 2022b). As of December 2022, 74 biosimilar medicines have been approved for use by the EMA and 40 have been approved by the U.S. Food and Drug Administration (FDA). Out of the EMA-approved biosimilars, nearly half (36) are monoclonal antibodies (EMA, 2022c; U.S. Food and Drug Administration [FDA], 2022).

1.2.1 IgG1

Antibodies are divided into five different isotypes: IgA, IgD, IgG, IgE and IgM (Nezlin, 1998). IgG is the most abundant type in the human serum and so far, IgGs have been the main focus of therapeutic antibody development (Hamilton, 1987; Irani et al., 2015). IgGs can be further classified into four subclasses called IgG1, IgG2, IgG3 and IgG4 (Nezlin, 1998). These IgG subclasses vary in structure, which impacts their function. While there is slight sequence variation in the heavy chain, resulting in some differences in exposed residues in the antibody surface, a large part of the variability between the IgG subtypes comes from the structure of the hinge region (Irani et al., 2015). The structures of the different IgG antibodies are illustrated in Figure 1.2.

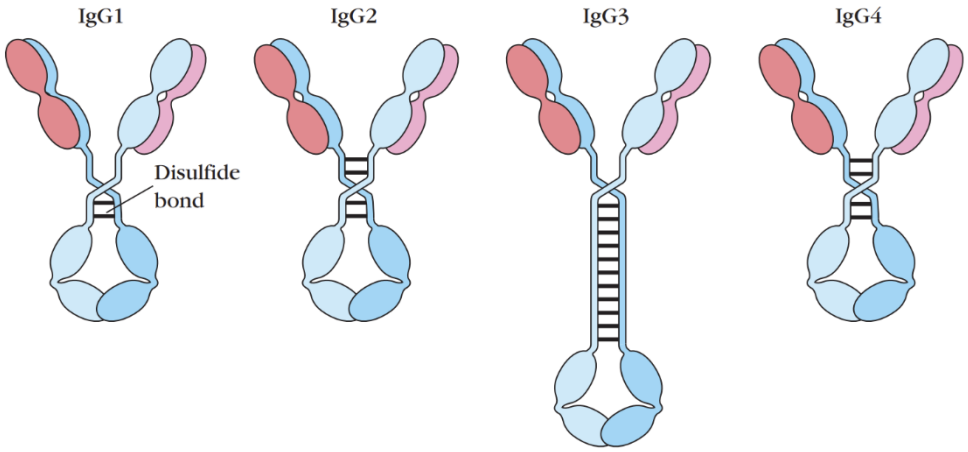

Figure 1.2 – Structure of the four IgG subclasses (Kindt et al., 2006).

For example, IgG3 has an exceptionally long hinge region that makes it difficult to purify, as it is more prone to degradation (Thomson, 2016). Moreover, IgG3 has a significantly shorter half-life than the other subclasses, making it less ideal for mAb development. The vast majority of approved mAbs are of IgG1 type, although several IgG2 and IgG4 mAbs have also been approved (Tang et al., 2021). The advantages of IgG1 for mAb development include its long half-life (which is comparable to that of IgG2 and IgG4), stability, as well as being less prone to aggregation as compared to the other subclasses. The hinge region of IgG1 is more flexible than the hinge regions in IgG2 and IgG4, which may be in part responsible for the decreased aggregation tendencies of IgG1 (Tang et al., 2021). IgG1 also has a higher binding affinity to the activating FcγRs as compared to IgG2 and IgG4, and it is able to effectively induce ADCC and antibody-dependent cellular phagocytosis (ADCP) (Yu et al., 2020).

Because of their size and complexity, including important post-translational modifications (PTMs) required for proper function, mAbs are produced in mammalian cell cultures (Fischer et al., 2015).

1.3 Cell lines

Bacterial and mammalian cell lines are commonly used as production platforms for biosimilars, although other cell types, such as plant or insect cells, can also be used. The choice of cell type depends on the characteristics of the product in question (Dumont et al.,

2016). The ideal cell line should be able to provide high yields, achieve high cell densities, low production of incorrectly processed proteins, and it needs to be able to produce protein-specific characteristics such as appropriate glycosylation patterns (Birch & Racher, 2006). Generally, bacterial cells are cheap options, they are able to grow to high densities and produce large quantities of the product. For simple biologics like insulin, bacterial cells such as *Escherichia coli* are a good option (Kesik-Brodacka, 2018). However, for more complex molecules, such as glycoproteins, bacterial cells may not be able to meet the expected quality criteria of the product. Today, the majority of biologics are produced with the use of mammalian cell lines (Birch & Racher, 2006).

1.3.1 Mammalian cell lines

In production of mAbs, mammalian cells are mainly used. The challenges of working with mammalian cells, as compared to bacterial cells, include slower growth rates, lower product yield, longer cultivation times and the need for expensive growth factors (Fischer et al., 2015). However, mammalian cells have the benefit of secreting the product directly out of the cells, removing the need for a lysis step during the purification process (Dumont et al., 2016). Also, they produce proteins that are similar to endogenous human proteins. One of the most widely used cell lines in mAb production is the Chinese hamster ovary (CHO) cell line (Kim et al., 2012). Like with any cell type used for production of biopharmaceuticals, CHO cells have been genetically engineered to optimize yields. Targets of genetic engineering include genes involved in cellular metabolism, apoptosis and glycosylation. This engineering involves knock-out of certain genes and overexpression of both endogenous CHO genes, as well as genes introduced to the CHO genome from other organisms (Fischer et al., 2015). Other types of cell lines widely used in mAb production include NS0 and Sp2/0 (murine myeloma cell lines) and baby hamster kidney (BHK) cells (Dumont et al., 2016).

1.3.2 Human cell lines

Human cells as production platforms for biopharmaceuticals are rapidly growing in popularity, but have not yet replaced cells such as CHO in the standard production system. As of 2016, two human cell lines, HEK293 and HT-1080, were being used to produce approved biologics (Dumont et al., 2016). A benefit of producing therapeutic proteins with

the use of human cells is that the risk of immunogenicity caused by non-human PTMs (and other potential endogenous host cell impurities) is eliminated. However, working with human cell lines also comes with challenges. For example, these cells may be prone to contamination with human viruses. Also, due to the long history of using non-human cells, there is simply more knowledge and understanding available when it comes to well established cell lines such as CHO (Dumont et al., 2016).

1.4 Upstream processes

1.4.1 Bioreactor process types

The initial stage of biopharmaceutical production, called upstream processing, involves everything from development of the cell line to the full-scale cultivation in bioreactors where the target protein is produced (Jungbauer, 2013). Several different types of bioreactor systems have been designed, including airlift reactors, wave-mixed bioreactors and stirred-tank bioreactors (Pörtner, 2015). The four main bioreactor process types for stirred-tank bioreactors are batch, fed-batch, continuous and perfusion processes (Mehra et al., 2017). Batch processes are the simplest of these, in which the cells are inoculated with all of the media they will require for the entire process. Batch processes typically last around 7 days, after which accumulation of byproducts and lack of nutrients lead to a drop in viability, preventing further culturing (Mehra et al., 2017). Fed-batch processes start out similarly to batch processes, but the feed containing the nutrients essential for the cells is continuously or semi-continuously added to the reactor based on regular monitoring of culture conditions (Lim & Shin, 2013). This allows the cell culture to survive and produce products for a longer amount of time, with typical fed-batch processes lasting around 14 days. This is the most commonly used method for large scale production of biopharmaceuticals nowadays, as it is relatively simple while still able to produce high product titers (Mehra et al., 2017). In both batch and fed-batch processes, the cells and the products stay in the reactor for the entire duration of the process. Continuous and perfusion cultures both involve addition of media and removal of products from the reactor during the production process, the difference being that in perfusion cultures, the cells are retained and returned into the bioreactor. Perfusion cultures allow for longer production times, contrary to batch and fed-batch processes, as

waste does not accumulate inside the reactor and cells remain viable for longer periods of time (Mehra et al., 2017).

1.4.2 Single use bioreactors and stainless steel bioreactors

Large scale production of mAbs (50 L – 20.000 L) takes place in bioreactors, which can be grouped into single use bioreactors (SUBs) and stainless steel bioreactors. In recent years, SUBs have been gaining popularity for manufacturing biopharmaceutical products. In these reactors, the culture is contained within a disposable bag, and after harvest, the bag is discarded. This allows for a quick turnaround time, as little time is required for cleaning and sterilization between batches. While they have higher consumable costs and are more reliant on suppliers for materials, they have significantly lower capital investments, making them a good option for new biopharmaceutical companies that have not already invested in stainless steel bioreactors (Shukla & Gottschalk, 2013). One limiting factor of SUBs is their working volume. Until recently, 2000 L SUB vessels were the largest on the market. However, recent developments have introduced SUBs with working volumes up to 5000 L (Thermo Fisher Scientific, 2021). Figure 1.3 shows the features of a 2000 L SUB from Thermo Fisher.

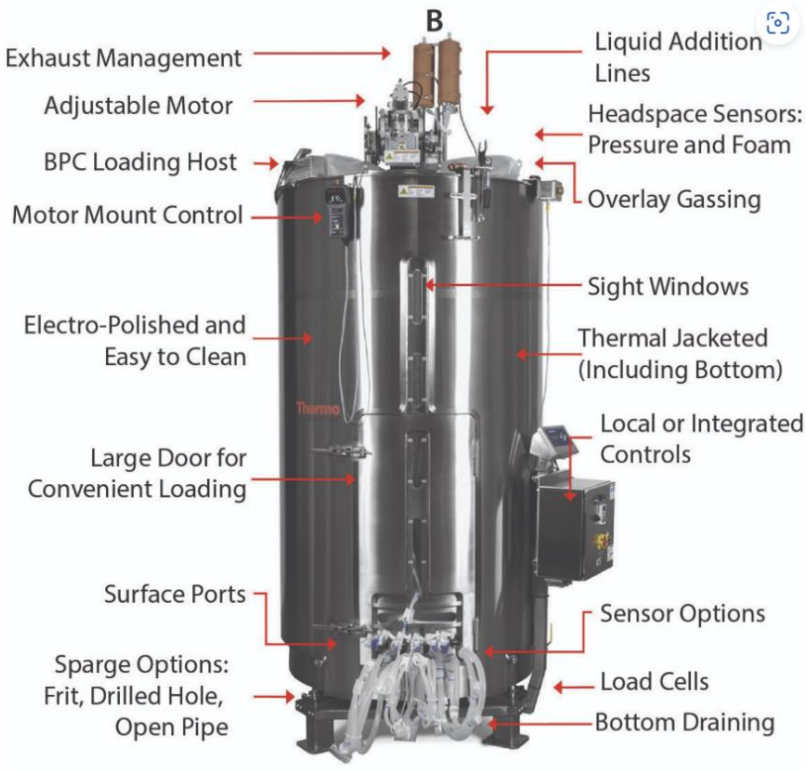

Figure 1.3 Thermo Fisher HyPerforma 2000 L SUB (Smith et al., 2018) .

Stainless steel bioreactors can reach much larger working volumes, up to 20,000 L. Since the cell culture is in direct contact with the reactor, as opposed to being contained in a disposable bag, the reactors require extensive cleaning and sterilization procedures after harvest, resulting in higher costs of cleaning materials as well as longer downtime between batches. There is also an increased risk of cross contamination if the same reactor is used to produce more than one product. However, neither SUBs nor stainless steel bioreactors can be regarded as superior to the other as the ideal bioreactor setup depends on many factors, including the product(s) being produced, previous equipment investments, required scale of production and long-term financial strategies (Rogge et al., 2015).

1.4.3 Harvest and downstream processes

A typical fed-batch process lasts around 14 days, after which the viability of the cell culture starts to decline. At this point, the cell culture is harvested, and the purification process of the harvest material is initiated. A clarification step, where the cells are separated from the rest of the material, is required before further purification. This is usually performed by either centrifugation or filtration. However, combining clarification and purification into one step is being researched as a time- and cost saving alternative (Brechmann et al., 2019). After clarification, the harvest material is put through a series of purification steps in order to ensure a pure final product. For most mAbs, the first step is Protein A chromatography. This affinity chromatography method is based on the high binding specificity of Protein A (a protein originally isolated from the bacterial species *Staphylococcus aureus*) to the Fc region of antibodies, resulting in the antibody being retained in the column while other materials flow through. Following this, polishing chromatography steps, including anion exchange and cation exchange chromatography, are used to remove remaining impurities such as host cell proteins, DNA, aggregates or leached Protein A. The final steps of the purification process includes viral inactivation and ends with ultrafiltration/diafiltration to concentrate the product and change the buffer into the final formulation buffer (Shukla et al., 2007).

1.4.4 Bioreactor analytics

During the production processes in bioreactors, it is necessary to monitor the culture conditions as much as possible. Analytics performed during a bioreactor run can be carried out either directly inside the bioreactor, called in-line analytics, via an on-line loop, or by

removing samples from the reactor and analyzing them manually in the lab, called offline analytics. The culture bags used in many stirred-tank SUBs have ports which allow sterile insertion of probes to monitor culture conditions during production. Dissolved oxygen (DO) concentration and pH are easily monitored in real-time using these probes (Jossen et al., 2019). Other key parameters, such as viable cell density (VCD) and the concentration of various metabolites, are typically measured offline. However, a variety of methods allowing in-line analysis of these parameters have been developed, and there is currently much interest in further optimizing these methods to allow for reliable in-line monitoring (Bergin et al., 2022).

Viable cell density

The amount of product produced depends on the number of viable cells present in the cell culture, as well as the cells‘ specific productivity (Q_p). The Q_p of the cell lines used in large scale production has increased significantly over the last two decades (Butler & Meneses-Acosta, 2012). The high-yielding cell lines used today are a result of cell line optimization, as well as a more in-depth understanding of the required media components and optimized feeding strategies to employ during production (Birch & Racher, 2006). As the viable cell density in the reactor is usually the main indicator of cell growth, it is highly important to monitor it during the upstream process (Metze, Ruhl, et al., 2020).

The growth phases in cell cultures are split into several stages, shown in Figure 1.4. After inoculation, there may be a short lag phase where little growth is observed, when the cells are adjusting to the new conditions in the bioreactor. Following this, the VCD starts rapidly increasing during the exponential growth phase, until a plateau is reached, called the stationary phase. The stationary phase involves a decrease in growth rate while still maintaining a relatively high viability (over 80%). Finally, the death phase begins once the VCD starts dropping rapidly (Rish et al., 2022).

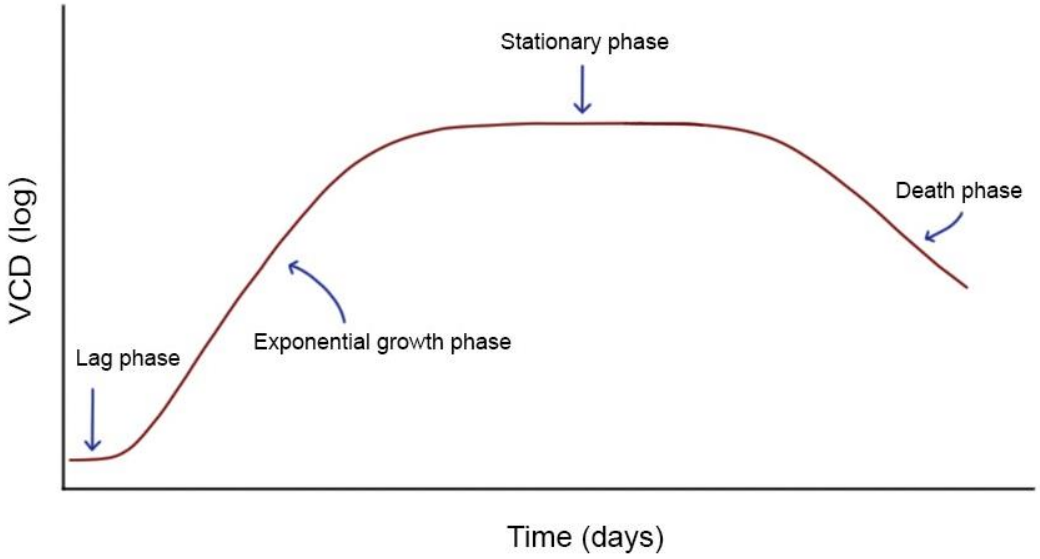

Figure 1.4 – Growth phases of cell cultures.

The VCD can be monitored offline by taking samples at regular intervals and using cell counting devices to assess the number of viable cells. This can be done by staining the cells using e.g. Trypan Blue dye, which is able to enter dead cells through their leaky membranes. Live cells are not stained as their membranes are intact. The VCD can then be determined based on microscopic image analysis. This offline cell counting method is simple and easy to perform. However, as more manual labor is required for offline monitoring of cell density, there is a larger potential for human error to occur during this process (Metze, Ruhl, et al., 2020). While offline sampling is still the main method for measuring VCD in the bioreactors, there has been a growing interest in the development of in-line methods for cell culture monitoring, that could enable real-time VCD determination.

1.5 Process analytical technology

In biopharmaceutical manufacturing, the goal is to develop a process that is able to consistently produce a high-quality product. In order to achieve this, regular monitoring of the process is important. Process analytical technology (PAT) is an initiative started by the FDA in 2004 that, based on continuous monitoring of the pharmaceutical production process, aims to allow control of the manufacturing to ensure a consistently high quality of

the final product (Rathore et al., 2010). In manufacturing, tools that allow real-time monitoring are ideal, as they allow for greater control of the production process. Since sampling is typically infrequent, e.g. once a day, important events in the process may not be detected for several hours. However, with in-line monitoring of important culture parameters, early detection of changes in the culture conditions may allow a faster response that could potentially save a production batch. A reduced need for sampling also decreases the risk of contamination, as any interaction with a closed reactor system introduces a certain level of risk (Metze, Ruhl, et al., 2020).

Implementation of PAT methods into bioprocesses comes with certain challenges. The bioreactor stage is where the quality of the product is largely determined, making it important to monitor this process. However, the environment within the bioreactor is complex, with a multitude of reactions occurring, and metabolites and nutrients being produced and consumed by the cells. As all of these factors can influence critical quality attributes of the product, development of tools that allow us to properly monitor the bioreactor environment is necessary (Streefland et al., 2013). As production of biopharmaceuticals is a sterile process, any sensors that are in direct contact with the culture must be aseptically introduced into the reactor or sterilized together with the reactor (Steinwedel et al., 2019).

1.5.1 PAT methods for VCD monitoring

Several methods have been developed to allow in-line monitoring of biomass in bioreactors, many of which are spectroscopic methods. For example, near-infrared (NIR) spectroscopy and Fourier-transform infrared (FTIR) spectroscopy are based on light absorption in different regions of the electromagnetic spectrum (Claßen et al., 2017). FTIR spectroscopy, using wavelengths in the mid-infrared region, results in spectra with bands of the fundamental vibrational transitions (Subramanian & Rodriguez-Saona, 2009). NIR spectra may have many overlapping bands due to molecules having multiple overtone and combination bands in the NIR region of the electromagnetic spectrum, making them more difficult to interpret (Camacho & Karlsson, 2001). Raman spectroscopy is another PAT method for in-line culture monitoring (Johansson et al., 2010). Whereas NIR and FTIR spectroscopy are based on optical absorption, Raman spectroscopy is based on inelastic scattering of monochromatic light by molecules (Long, 1971). As light hits the molecule, it is absorbed and reemitted. While most of the reemitted light remains at the original

wavelength, a small portion of the light is reemitted at a different wavelength, which is specific to the molecule (due to its molecular structure and bonds). Using the FTIR, NIR or Raman spectra, in combination with chemometric tools such as partial least squares (PLS) and principal component analysis (PCA), it is possible to develop models that allow for real-time monitoring of metabolite concentrations, as well as cell density (Abu-Absi et al., 2011; Challa & Potumarthi, 2013). Dielectric spectroscopy, or capacitance, can also be used to estimate VCD in real-time.

1.5.2 Capacitance

In-line VCD monitoring using capacitance measurements is a highly promising method. The principle of the method is based on the cells' ability to become polarized due to their plasma membranes separating them from the external environment (Carvell & Dowd, 2006). When a capacitance probe applies an electric field to the suspension, positively charged ions within the cells move towards the field, and negatively charged ions move away from it. As the cell membrane is composed of a non-conducting phospholipid bilayer which is impermeable to charged particles such as ions, the ions accumulate at the poles, resulting in polarization of the cell (Carvell & Dowd, 2006; Kulbacka et al., 2017). This polarization can be measured by capacitance probes, illustrated in Figure 1.5.

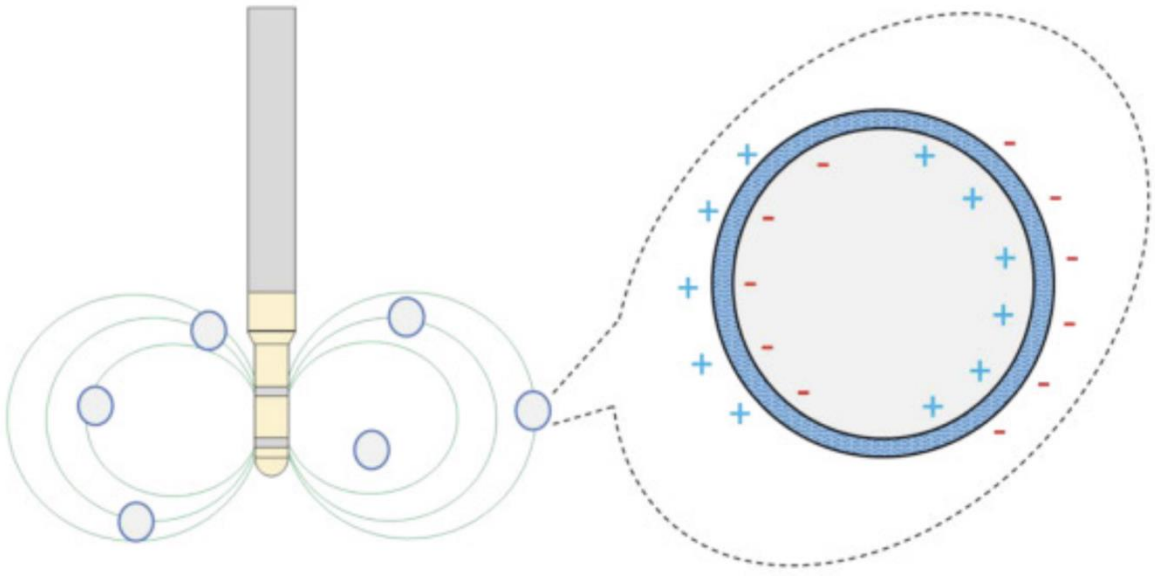

Figure 1.5 – Polarization of live cells due to electric field emitted by a capacitance probe (Bergin et al., 2022).

As dead cells do not have intact cell membranes, they contribute much less to the capacitance measurements. Other non-cell materials found in the solution, such as debris, air bubbles or oil droplets, do not contribute either, as they do not have membranes and thus cannot be polarized. With increased cell concentrations in the solution, the capacitance increases, as more cells are becoming polarized and contributing to the readings (Carvell & Dowd, 2006).

The capacitance is measured in Farads (F), typically pico-Farads (pF). The measured capacitance values (C_m) can be converted into VCD values by multiplying them with the biomass factor:

$$VCD = C_m \times biomass\ factor$$

The optimal biomass factor varies depending on the cell line being used, so it is important to determine it for each process.

Capacitance probes can take readings multiple times per minute, thus giving real-time feedback on the VCD. As VCD is a key indicator of culture conditions and considering the importance of PAT implementation in the bioprocesses, capacitance measurements are becoming a popular method for in-line VCD determination. This method remains accurate until the cell culture reaches the end of the production phase. When cells go through apoptosis, stress may cause their cell diameter to change. As larger cells contribute more to the capacitance measurements, the readings taken during the death phase are no longer relative to the VCD (Bergin et al., 2022).

Figure 1.6 shows an example of a capacitance trend during a 14 day fed-batch process. Shortly before inoculation, the capacitance value is set to zero so that all changes in capacitance readings are caused by the cells. Starting from day 3, small dips can be observed in the graph at regular intervals. This corresponds to the daily feeding, as the culture gets slightly diluted each time feed is added.

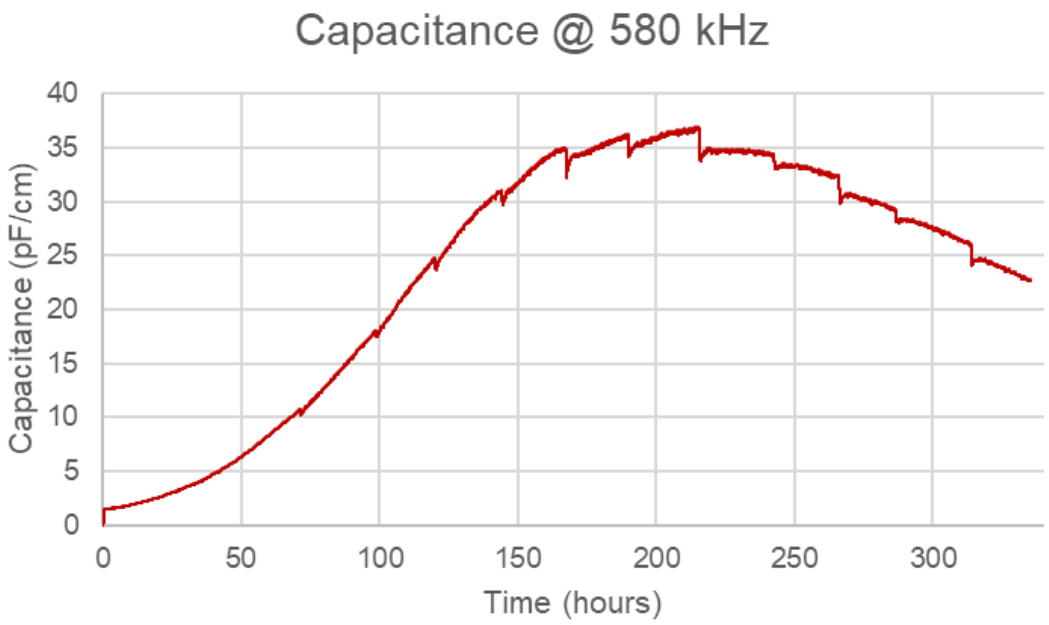

Figure 1.6 Example of a capacitance trend during a 14-day fed-batch process.

Recent research has explored the reliability of capacitance measurements for VCD determination across various scales, ranging from 50 L bioreactors up to 2000 L bioreactors. The results showed that during the exponential growth phase, capacitance was a reliable determinant of VCD across all scales, with coefficients of determination (R^2) of 99% or higher during the exponential growth phase at every scale (Metze, Blioch, et al., 2020).

A benefit of this method is the simplicity of the data processing needed to correlate capacitance to VCD – linear regression models can be used to interpret single-frequency capacitance data. Moreover, when measuring capacitance at a range of different frequencies, and applying more complex data analysis techniques, it is possible to gain a more detailed insight into the culture conditions (Bergin et al., 2022).

Frequencies

Capacitance measurements can be carried out either at a single frequency or multiple frequencies. The simplest utilization of capacitance measurements involves measuring at a single frequency for the entire process. The main downside of this is that it does not distinguish between increased VCD and increased cell diameter, as both of these factors lead to increased values in capacitance readings. Single frequency measurements essentially measure the viable cell volume (VCV), which is why it is only accurate during the

exponential growth phase, when cell diameter remains relatively stable (Metze, Ruhl, et al., 2020).

The frequency used depends on the cell type. As bacterial cells are smaller, higher frequencies are typically used (1000 kHz), whereas for mammalian cells, frequencies around 500-600 kHz are used. By measuring additionally at an overly high frequency, above 10 MHz, it is possible to correct for baseline shifts that may occur during the process by subtracting the high-frequency measurement from the working frequency measurement (Dabros et al., 2009).

The frequency used, in combination with the cell size, impacts the capacitance measurements. At higher frequencies, there is less time for the cells to polarize, resulting in lower capacitance measurements if the cells do not manage to polarize entirely (Carvell & Dowd, 2006). However, the time needed for cells to polarize depends on their size, with smaller cells requiring less time for complete polarization (Metze, Blioch, et al., 2020). This phenomenon, where cells lose the ability to polarize as frequency increases, is called β-dispersion and is illustrated in Figure 1.7.

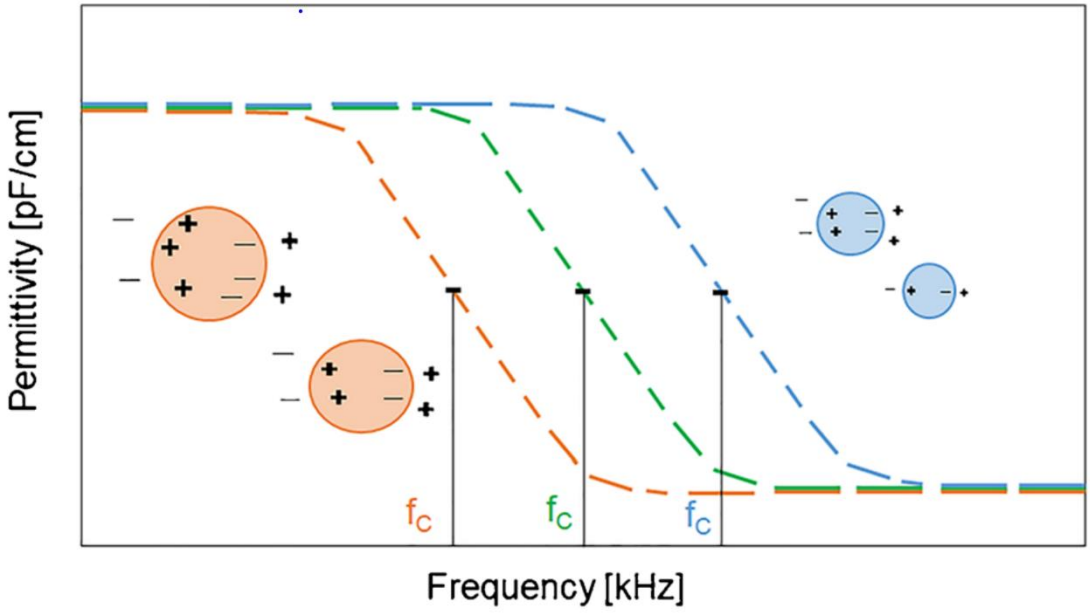

Figure 1.7 - β-dispersion curve. Large cells, shown with an orage line, have a low f_c. As cells get smaller, the f_c value becomes larger, as they need less time to polarize completely (Metze, Blioch, et al., 2020).

At low frequencies, the cells will always reach complete polarizaton (low-frequency plateau) and at high frequencies, no cells polarize (high-frequency plateau). All cells have a characteristic frequency (f_C), where the rate of polarization is halfway between the low- and

high frequency plateaus (Metze, Blioch, et al., 2020). This parameter can be used to gain further insight on culture conditions using frequency scanning.

Frequency scanning has the ability to provide in-line VCD measurements while also being able provide additional information on the physiological state of the cells. Rather than taking measurements at one single frequency, measurements are taken at multiple frequencies each time, called capacitance frequency scanning. However, compared to single frequency capacitance measurements, this requires significantly more complex data analysis in order to interpret the results (Ansorge et al., 2010).

The f_C can shift during the process due to a variety of factors, including changes in cell size or intracellular conductivity (σ_i). Ansorge et al. found that when a CHO cell culture experienced nutrient limitations (glutamine depletion) during the shift from the exponential growth phase to the stationary phase, the f_C dropped. This was concluded to be due to changes in σ_i. Thus, multifrequency scanning may be useful in monitoring the intracellular state of the cells, as changes in f_C can indicate changes in nutrient availability (Ansorge et al., 2009).

Conductivity

Capacitance probes also measure conductivity in the culture. Morris et al. used real-time conductivity trends to detect signs of bacterial contamination in bioreactors. Typically, the conductivity increases in small steps throughout the process. However, upon contamination a sharp increase was detected. This abnormality occurred hours before other contamination signs including pH and DO drops, showing that conductivity may be used for early detection of contamination (Morris et al., 2021).

2 Aim of this project

In Alvotech, VCD is currently measured offline once a day, in the ViCell BLU Cell Viability Analyzer. There are many opportunities for operator errors to occur, such as during sampling, diluting, analysis and data processing, potentially impacting the quality of the batch if changes are made to the process based on inaccurate cell counts. Real-time monitoring tools reduce the risk of such errors by providing additional information about the process. Up to date, capacitance meansurements are not yet used in any process control in Alvotech.

The aim of this project is to investigate the use of capacitance probes for the generation of batch fingerprints that can be used for real-time cell growth monitoring. Specifically, generic batch fingerprints for VCD will be developed based on capacitance measurements. Additionally, the biomass factor used to convert capacitance measurements into cells/mL will be optimized. Scalability of capacitance trajectories between different scales (15 L, 50 L and 250 L) will also be investigated.

3 Methods and materials

3.1 15 L bioreactor setup

3.1.1 Bioreactor preparation

For each 15 L bioreactor run, two 15 L HyPerforma Glass Bioreactors (Thermo Scientific) were used. The glass vessel and the headplate were washed, before wiping the headplate down with isopropyl alcohol (IPA) and installing it into the bioreactor. Sterile tubing manifolds were prepared and attached to the headplate, with all ends of tubing being attached to 0.2 µm hydrophobic vent filters (Cytiva). The probes (pH, DO, capacitance and Raman) were prepared and inserted into the reactor, which was then autoclaved. Pressure tests were performed before and after autoclaving, to ensure that there was no leak in the system.

pH was measured in-line using the InPro 3253i SG/425 pH probe (Mettler Toledo) and DO was measured in-line using the InPro6860i/12/320/nA/HD DO sensor (Mettler Toledo). Raman spectra were acquired using bIO-Optic (Endress+Hauser) with the Raman Rxn-10 probe (Endress+Hauser).

On the day before inoculation, the bioreactor was filled with ActiPro™ Seed Train & Bioreactor Media (Cytiva) and allowed to reach 37°C. FoamAway™ Irridated AOF Antifoam (Thermo Fisher Scientific) and 0.5 M NaOH were welded on to their respective lines. All other additions (450g/L D-Glucose (Cytiva) and BalanCD CHO Feed 4 (FUJIFILM Irvine Scientific) for mAb 1, and L-glutamine (Merck), Cell Boost 7a (Cytiva) and Cell Boost 7b (Cytiva) for mAb2) were welded to their respective addition lines at any time before the first addition was needed. During the bioreactor runs, glucose, BalanCD CHO Feed 4, glutamine, Cell Boost 7a and Cell Boost 7b were placed on a scale to allow for addition into the bioreactor based on scale weight.

3.1.2 Capacitance probes

Futura 12 x 450 mm annular probes from ABER Instruments were used in the 15 L bioreactors. The software FuturaTool 3.0.4.0 (Aber Instruments) was used for capacitance measurements. Figure 3.1 shows the capacitance probe used in the 15 L bioreactors.

Capacitance data was also gathered from several 250 L batches running alongside the 15 L batches. In the 250 L SUB, Futura 12 x 220 mm annular probes from ABER Instruments were used.

Prior to installation of the probes in to the bioreactors, signal simulator tests were performed with a zero signal simulator (0pF/cm, 0mS/cm) and a high signal simulator (100pF/cm, 40mS/cm). A standard conductivity test with 0.1 M KCl solution was then performed. The Futura probe was then removed and replaced with a protection cap for autoclaving.

Once the reactor had been autoclaved and filled with media, the capacitance probe was connected to the Aber Connect (Standard Remote Futura). Readings were carried out for the entire duration of the process, with the probe taking measurements at approximately 30 second intervals.

The following settings were used for the capacitance measurements:

- Measuring frequency: 580 kHz
- High frequency: OFF
- Filter: 30
- Polarisation correction: B220 PolC
- Measurement type: Scans

Figure 3.1 - Futura 12 x 450 mm probe used in 15 L bioreactor batches.

Additional capacitance data for mAb1 (see 3.1.3) was received from previous bioreactor runs in the Alvotech Pilot Lab, in 15L, 50L and 250L bioreactors.

3.1.3 Inoculation

Two cell lines producing two different IgG1 mAbs were used in this project. They will be referred to as mAb1 and mAb2. The cells used in the 15 L batches were obtained from the N-1 stage intended for the inoculation of the 250 L batches running at the same time. The amount of cell culture used to inoculate the reactors was calculated based on the VCD of the N-1 stage culture, in order to achieve a starting VCD of 0.5E+06 or 0.7E+06 cells/mL.

The N-1 stage of the cell culture was derived through a series of cell passages, or seed train, starting with the thaw of a frozen vial containing the cells used to inoculate the first culture stage (N-6). The stages of the seed train are listed in Table 3.1.

Table 3.1 – Seed train stages in the generation of the cell culture used to inoculate the 15 L bioreactors

Seed train stage	**Working volume**	**Target starting VCD (cells/mL)**	**Target starting viability**	**Culture duration (hours)**
N-6: 1 x 125 mL shake flask	30 mL	$\geq 0.20 \times 10^6$	≥ 80.00 %	96 ± 4
N-5: 1 x 500 mL shake flask	125 mL	$0.30 \times 10^6 \pm 0.10 \times 10^6$	≥ 85.00 %	96 ± 4
N-4: 1 x 2000 mL shake flask	700 mL	$0.50 \times 10^6 \pm 0.10 \times 10^6$	≥ 85.00 %	72 ± 4
N-3: 4 x 2000 mL shake flasks	700 mL	$0.50 \times 10^6 \pm 0.10 \times 10^6$	≥ 85.00 %	72 ± 4
N-2: 1 x 50L SmartRocker (Finesse)	10 L	$0.50 \times 10^6 \pm 0.10 \times 10^6$	≥ 85.00 %	72 ± 4
N-1: 1 x 50L HyPerforma Single-use Bioreactor (Thermo Fisher Scientific)	40 L	$0.50 \times 10^6 \pm 0.10 \times 10^6$	≥ 90.00 %	72 ± 4

The complete bioreactor setup is shown in Figure 3.2. The reactors are covered due to the inclusion of Raman probes in the experiments.

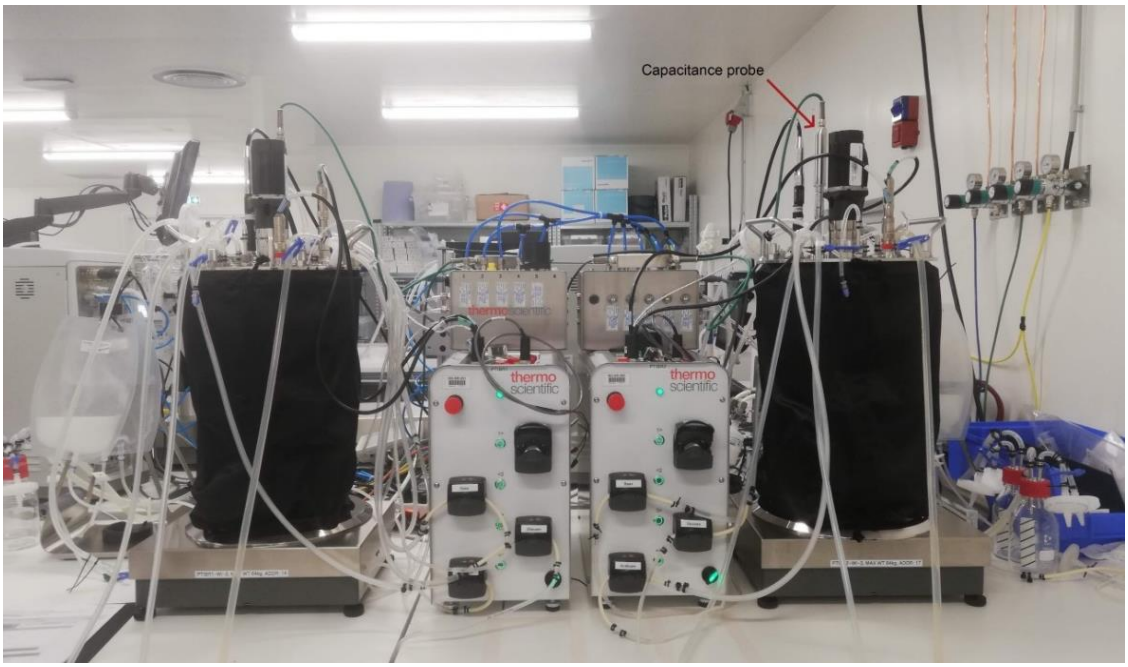

Figure 3.2 – Setup of 15 L bioreactors used in this study.

3.2 Daily sampling

3.2.1 Parameter check

Sampling was performed once per day. Important parameters were checked to ensure they were within the acceptable limits, which are shown in Table 3.2. The trends for these parameters over the past 24 hours were also assessed to see if any anomalies had occurred since the previous sampling.

Table 3.2 – Parameters checked before daily sampling.

Parameter	Target range for mAb1	Target range for mAb2
Temperature	37.0 ± 1.0°C	37.0 ± 1.0°C
pH	7.00 ± 0.25	7.00 ± 0.25
DO_2	30% ± 10%	30 ± 10 %
Agitator	200 ± 5 RPM	180 ± 5 RPM
Air flow	0.20 L/min	0.50 L/min

All data sampling was recorded in the batch record and in the batch data sheets.

3.2.2 Sampling

Sampling was done using a sterile 20 mL syringe. Prior to sampling, the syringe tip and sample port were sprayed with IPA. 20mL of culture was removed to flush the line, ensuring the sample analyzed was representative of culture conditions. Using a new syringe, 7-8 mL of culture was removed for analysis.

3.2.3 Offline pH

The pH was measured immediately after sampling, using the SevenExcellence pH meter (Mettler Toledo). Depending on the outcome, the following actions were taken:

Difference between online and offline pH <0.05: No action

Difference between online and offline pH 0.06 - 0.10: 1-point standardization of the in-line probe performed

Difference between online and offline pH >0.1: Re-sample (if difference is still >0.1, perform 1-point calibration)

3.2.4 Offline osmolality

Osmolality was measured using the OsmoTECH® PRO Osmometer (Advanced Instruments). 1 mL of the cell culture was put into an Eppendorf tube and centrifuged at 2.7k*g for 5 minutes. The cell pellet was discarded and 30 µL of the supernatant put into the sample tube for measurement.

3.2.5 Offline VCD

Offline VCD for mAb1 was measured using both ViCell BLU Cell Viability Analyzer (Beckman Coulter Life Sciences) and NucleoCounter® NC-202™ (ChemoMetec). Prior to analysis, 1 mL of cell culture was put into an Eppendorf tube, which was inverted several times to ensure a homogeneous culture. For ViCell BLU analysis, 200 µL of culture were removed from the Eppendorf tube and placed into a sample tube. For NucleoCounter

analysis, a Via2-Cassette™ (ChemoMetec) was used to obtain the culture sample from the Eppendorf tube. Measurements from ViCell BLU were used for further calculations.

For mAb2, Cedex HiRes Analyzer (Roche) and NucleoCounter® NC-202™ were used, with Cedex HiRes Analyzer results being used for further calculations.

If VCD was equal to or higher than 1×10^7 cells/mL, the samples were diluted 1:1 with PBS (1X, pH 7.4) prior to measuring.

3.2.6 Offline metabolite analysis

Metabolite concentrations were measured using the Cedex Bio Analyzer (Roche). 1 mL of the cell culture was put into an Eppendorf tube and centrifuged at 2.7g for 5 minutes. The supernatant was poured into a new Eppendorf tube and the cell pellet was discarded. The tube containing the supernatant was then placed in the Cedex Bio Analyzer. Depending on the day, the following metabolites were measured:

Day 0 – Day 3: Glucose, ammonia, glutamine, glutamate, lactate.

Day 4 – Harvest: Glucose, ammonia, glutamine, glutamate, lactate, IgG, lactate dehydrogenase (LDH).

3.2.7 Feed additions

For mAb1, glucose and BalanCD CHO Feed 4 were used.

Glucose was added on days where the concentration was measured below 3 g/L. Glucose was added to bring the concentration up to 6 g/L.

Starting from day 3, BalanCD CHO Feed 4 was added to the reactor daily based on weight (prior to glucose addition) with the following guidelines:

Day 3 – Day 5: Add 2% of bioreactor weight

Day 6 – Day 9: Add 3% of bioreactor weight

Day 10 – Day 13: Add 2% of bioreactor weight

For mAb2, L-glutamine, Cell Boost 7a and Cell Boost 7b were used.

Starting from day 2, glutamine was added on days where the concentration was measured below 2 g/L, according to the following formula:

$$Glutamine\ addition\ (kg) = 2 \times \frac{Bioreactor\ weight(kg)}{212.40}$$

Where:

212.40 = concentration (mM) of the L-glutamine used.

Starting from day 3, Cell Boost 7a was added every other day based on a set percentage of bioreactor weight:

- Day 3, day 9 and day 11: 3.080% of bioreactor weight
- Day 5 and day 7: 4.620% of bioreactor weight

Starting from day 3, Cell Boost 7b was added every other day based on a set percentage of bioreactor weight:

- Day 3, day 9 and day 11: 0.310% of bioreactor weight
- Day 5 and day 7: 0.460% of bioreactor weight

3.2.8 Antifoam addition

During daily sampling, the level of foam in the bioreactor was assessed visually. If a certain amount of foam had accumulated, a few drops of antifoam were added.

3.2.9 Pressure buildup

In batches mAb1-001A and mAb1-001B, four Acro50 exhaust filters (Pall Laboratory) were used for each bioreactor, with one being open at a time. When pressure buildup was detected in the bioreactor, the filter connected to the exhaust line was switched out by unclamping the tube to an unused filter and clamping off the used filter. In the following 15 L batches, only one filter was used, which did not need to be exchanged during the process.

3.3 Harvest

The harvest criteria for batches mAb1-001A&B were 70% viability or 14 days of culturing, whichever occured first. The other batches were not harvested. Instead, the cells were inactivated by adding NaOH pellets for a final concentration of 0.2-0.3 M base, and letting the base solution run for 24-48 hours before discarding the material.

3.4 Data processing

All capacitance data was converted into VCD predictions by multiplying the capacitance measurements with the biomass factor:

$$VCD = C_m \times biomass\ factor$$

The biomass factor was calculated using the following formula:

$$Biomass\ factor = \frac{Known\ cell\ concentration\ \left(\frac{cells}{mL}\right)}{Capacitance\ reading\ \left(\frac{pF}{cm}\right)}$$

Data processing was performed using Excel® (Microsoft Corporation). The coefficient of determination (R^2) used in the linear regression models was found using Excel, which uses the following formula:

$$R^2 = \frac{n(\Sigma xy) - (\Sigma x)(\Sigma y)}{\sqrt{[n\Sigma x^2 - (\Sigma x)^2][n\Sigma y^2 - (\Sigma y)^2]}}$$

The variables x and y represent the capacitance measurements in pF/cm and offlince VCD measurements in cells/mL, respectively.

4 Results & Discussion

4.1 Capacitance trends

All capacitance data used here was measured at 580 kHz. VCD predictions based on capacitance measurements were generated for all batches, 14 of which were mAb1 processes and 3 were mAb2 processes. Two biomass factors were calculated for each batch, one based on measurements from the entire process, and one based solely on the exponential growth phase. Figure 4.1 shows the capacitance trend for mAb1-001b (Figure 4.1 a), and VCD predictions using the biomass factor calculated for this run utilizing measurements from the exponential growth phase (Figure 4.1 b). Figure 4.1 b shows the VCD trajectory, represented in cells/mL, following inoculation. The VCD increases rapidly during the exponential growth phase, until a peak VCD of 1.29E+07 (1.25E+07 according to capacitance-based VCD prediction) is reached on day 7. Following this, the VCD slowly declines during the stationary and death phases. Small dips occur at regular intervals, representing the feed additions, as the culture gets slightly diluted as a result of feed addition.

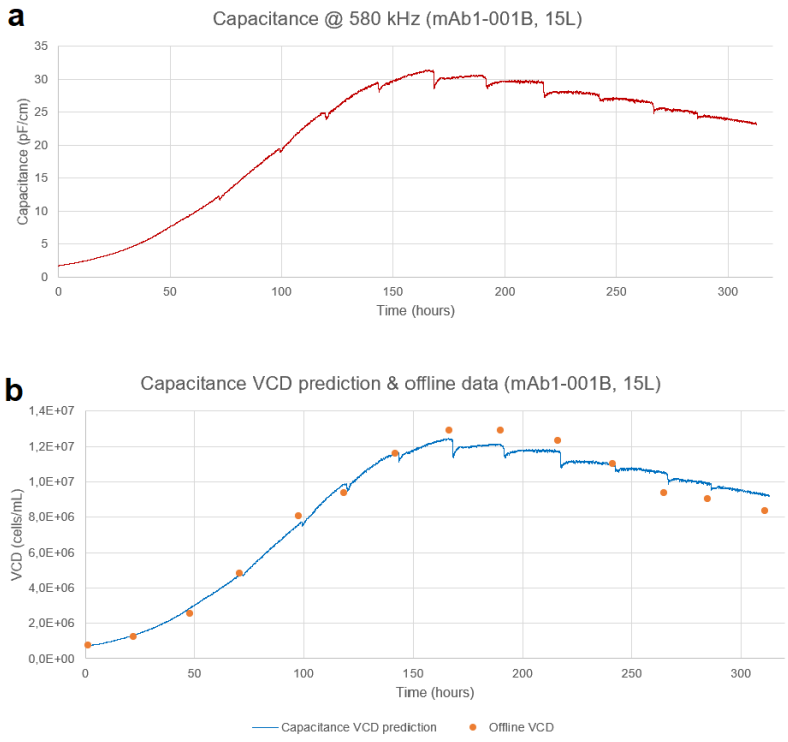

Figure 4.1 – (a) Capacitance trend for mAb1-001b. (b) VCD prediction based on capacitance measurements (blue line) and offline VCD measurements (orange circles).

It is clear that during the exponential growth phase, the VCD predicted by capacitance measurements accurately represents the VCD. During the later stages of the process, however, the VCD prediction becomes less accurate, consistent with results from similar experiments (Cannizzaro et al., 2003; Metze, Ruhl et al., 2020; Opel et al., 2010). A similar trend was observed in all batches, with VCD generally being overestimated after the end of the exponential growth phase for mAb1. This can happen as a result of increased cell diameter, as each cell would then contribute more to the capacitance measurements leading to an overestimation of cell density. During these later stages of the cultivation process, stress responses can get triggered in the cells, causing them to increase in size. For mAb2, however, the VCD seems to be underestimated during this time. Figure 4.2 shows VCD predictions for two batches of mAb2, one 15 L and one 250 L batch, using the specific biomass factors generated for each batch. As there were only three batches of mAb2, it is difficult to draw conclusions from this data, especially since several of the offline VCD data points were questionable (see Figure 4.2 b).

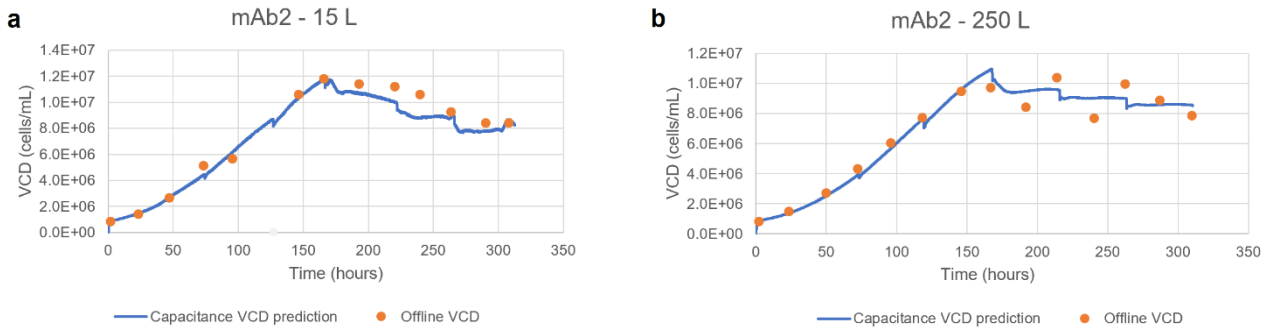

Figure 4.2 – (a) VCD prediction for mAb2-003A (15 L). (b) VCD prediction for mAb2-041 (250 L). Offline data points are shown with orange circles.

4.1.1 Capacitance trends for mAb1 - 15 L processes

In settings where optimal process performance is crucial, such as during manufacturing or in consistency and stability studies in process development, having a process-specific fingerprint to which each batch can be compared to is extremely valuable. The fingerprint, a.k.a. the golden batch trajectory, can be developed using either data from offline sampling or from real-time monitoring. As data capture is much more frequent using real-time monitoring, the resulting batch fingerprint is more accurate. This golden batch trajectory is based on successful runs of a specific process, allowing quick identification of deviations in

any following batches, which enables immediate action to be taken to try to recover the process.

Figure 4.3 shows the capacitance trends for all mAb1 processes tested here at the 15 L scale. Generally, they followed a similar trend, especially during the exponential growth phase. Two batches, mAb1-024 and mAb1-027B, have a noticeably different trend during the exponential growth phase. This is due to the fact that during the first few days of the process, the cell growth was slower, as compared to the rest of the batches. This difference can be explained by a process change, as these two batches had a lower seeding density (0.5E+06 cells/mL) than the rest of the batches (0.7E+6 cells/mL), resulting in a slightly delayed increase in capacitance.

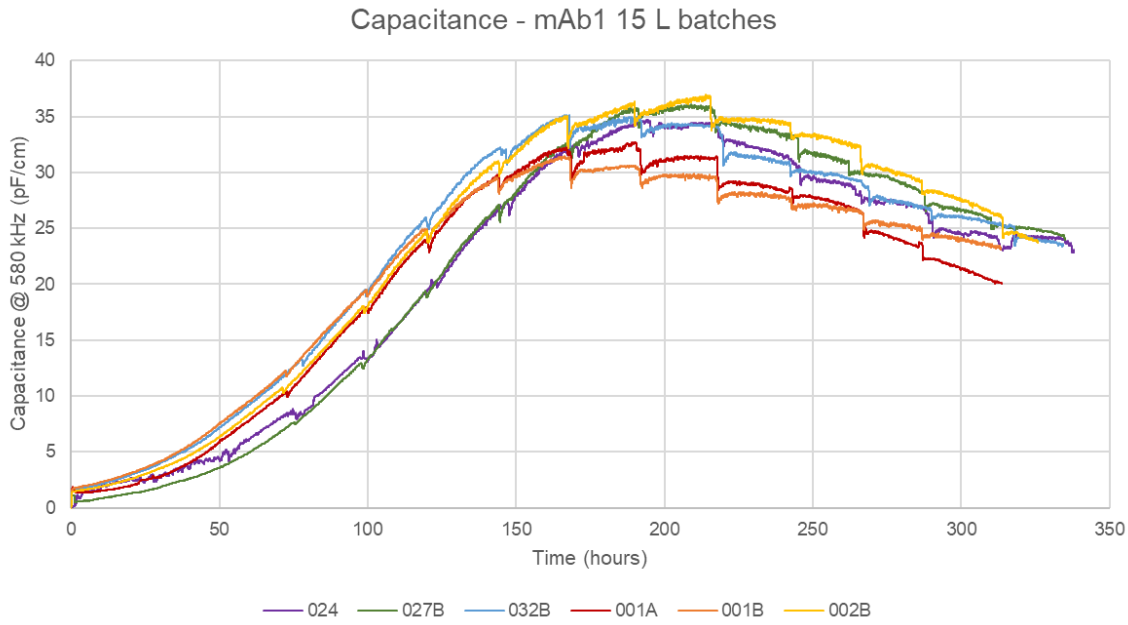

Figure 4.3 – Capacitance trends for all the tested 15 L batches of mAb1.

There is more variation in the capacitance trends during the second half of the cultivation. This lack of uniformity is largely explained by the batches simply having more variability in offline VCD during this stage. In both offline data and the capacitance trajectories, the batches follow a more similar trend during the exponential growth phase, and exhibit more variation during the stationary and death phases. This is shown in figure 4.4, where the in-line VCD predictions and offline VCD measurements were compared for four batches of mAb1 (three 15 L and one 250 L). One exception to this is mAb1-001A, which has lower capacitance readings than expected compared to its offline VCD. However, investigation of the capacitance data for this batch revealed that the capacitance readings did not properly

stabilize before zeroing the readings prior to inoculation, potentially causing slightly inaccurate readings throughout the process.

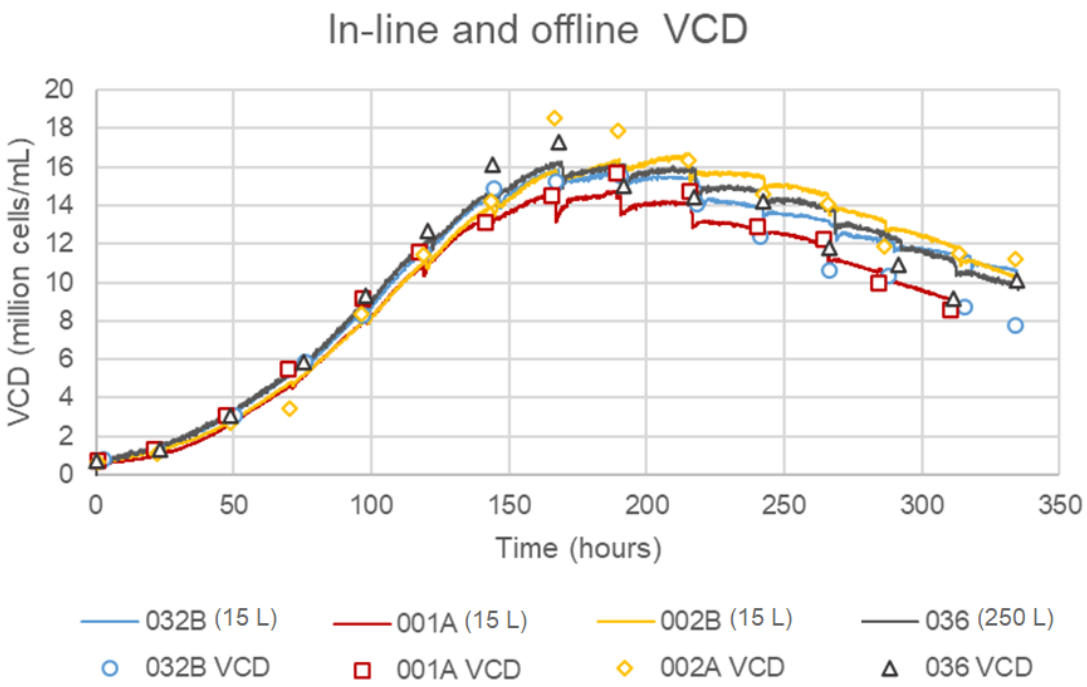

Figure 4.4 – In-line and offline VCD for four batches of mAb1. The lines represent VCD predictions based on capacitance measurements and offline VCD measurements are represented by markers. The batches shown are mAb1-032B (15 L, shown with a blue line and blue circles), mAb1-001A (15 L, shown with a red line and red squares), mAb1-002B (15 L, shown wuth a yellow line and yellow diamonds) and mAb1-036 (shown with a grey line and grey triangles). All VCD predictions were calculated using the generic biomass factor generated for mAb1.

4.1.2 Capacitance trends for mAb1 - 250 L processes

Figure 4.5 shows the capacitance trends for all 250 L batches of mAb1. mAb1-025 had the same seeding density as mAb1-024 and mAb1-027B, which explains the delay in capacitance increase. The unusual dip in the capacitance trend observed at around 70 hours for this batch is presumably caused by something interfering with the capacitance measurements, such as an air bubble attached on the probe tip. Since the capacitance readings go back to the original trajectory following this dip, and it does not seem to affect the overall capacitance trend for the batch, its effect will be omitted. mAb1-030 and mAb1-036 follow a highly similar trend. The capacitance readings for mAb1-036 batch are quite noisy, which may indicate an issue with the readings, potentially a result of the bellow being incorrectly placed in the SUB and covering the measuring surface, rather than a reflection of the culture conditions.

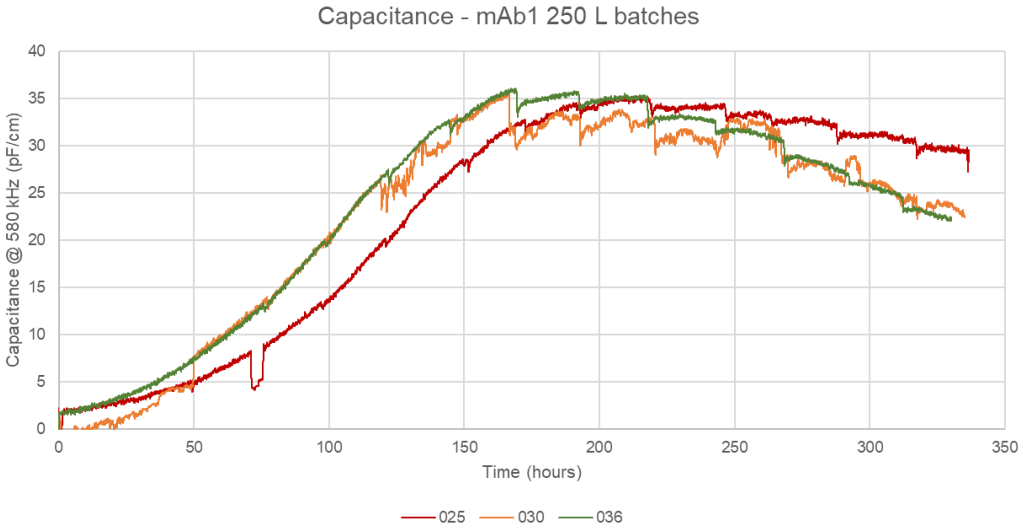

Figure 4.5 – Capacitance trends for all 250 L batches of mAb1.

4.1.3 Capacitance scalability of the mAb1 process

In process development, scalability of the process is important. While early development is typically done at a smaller scale, the process eventually needs to be scaled up to the final production volume. During scale-up, many parameters need to be considered to ensure consistent process performance at any scale, including working volume, stirring speed, oxygen transfer rate and homogenization time. Therefore, utilizing in-line monitoring tools, such as capacitance, to continuously monitor culture performance, we are better able to assess the success of process scale-up. We can also use these tools to identify whether/where potential problems with scale-up can occur.

Success of the scale-up strategy of the mAb1 process was investigated by comparing capacitance trends across three different scales. Figures 4.6 and 4.7 show the capacitance trends of mAb1 processes at 15 L, 150 L and 250 L. Figure 4.6 excludes the batches with a lower seeding density, so that all batches in this scalability investigation represent a similar process. The capacitance trends of the batches with a lower seeding density, including the 50 L batch, are shown in Figure 4.7. Both of these graphs indicate that the mAb1 process is scalable. While there is some variability between batches after the exponential growth phase, this variability does not seem to be dependent on scale, as there appears to be no systematic difference between the two scales. This variability can largely be explained by differences in offline VCD – the main exception being mAb1-001A, which had lower capacitance

measurements than expected based on offline VCD. These scalability results are similar to those described in the literature. Mezte, Ruhl et al. (2020) found similar results when investigating scale-up from 50 L to 2000 L in two different CHO cell processes, with no scale-dependent differences in capacitance trajectories.

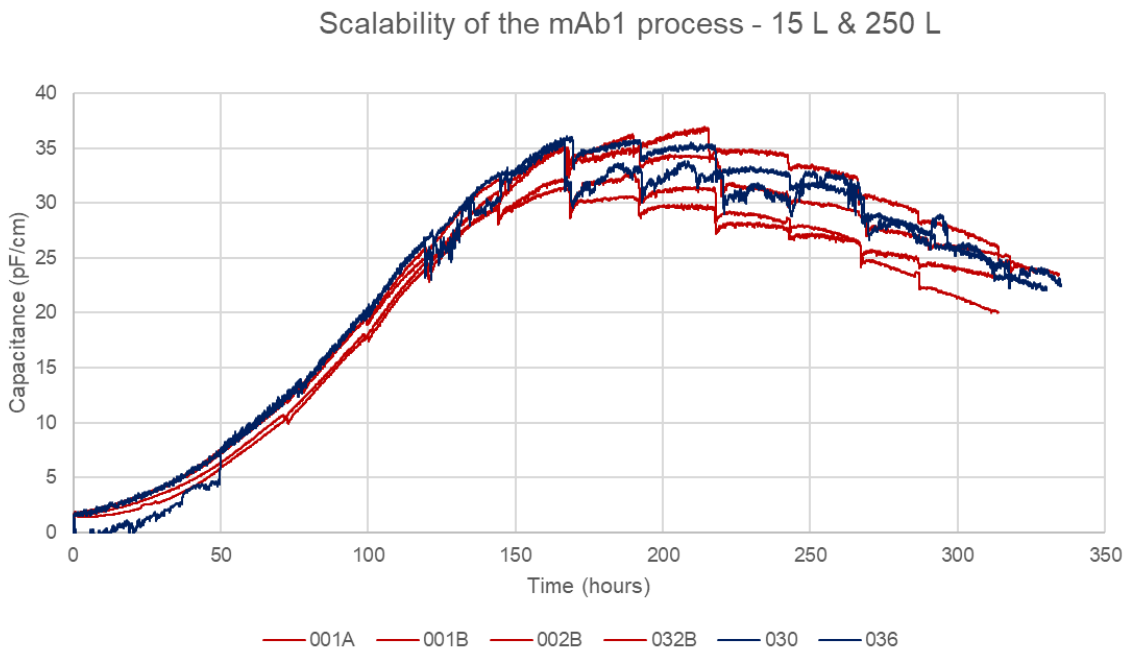

Figure 4.6 – Capacitance trends for mAb1 batches with a seeding density of 0.7E+06 cells/mL. 15 L batches are shown in red and 250 L batches are shown in blue.

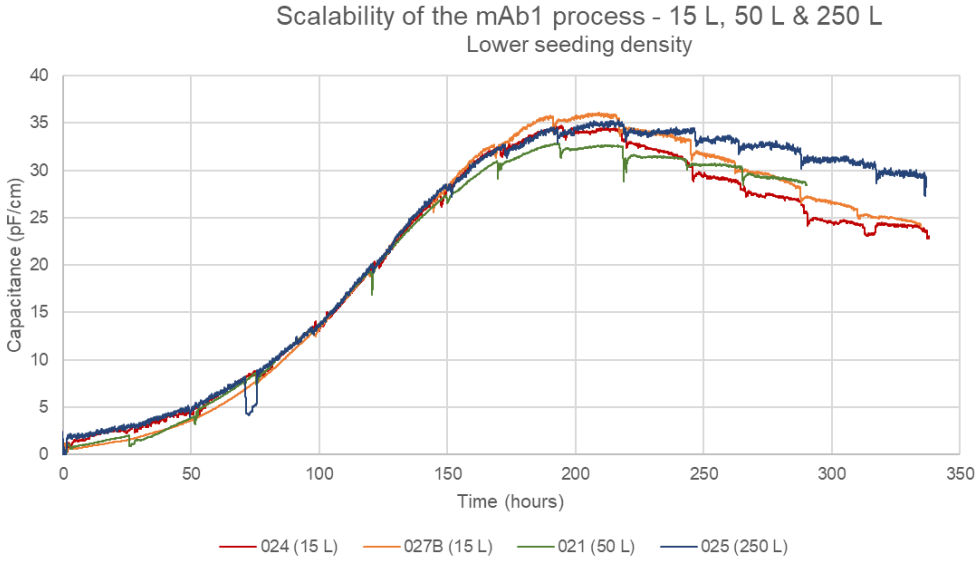

Figure 4.7 – Capacitance trends for mAb1 batches with a seeding density of 0.5E+06 cells/mL, at three different scales: 15 L (red and orange), 50 L (green) and 250 L (blue).

4.1.4 Capacitance trends and scalability for mAb2 – 15 L and 250 L processes

Capacitance data for mAb2 was collected for two 15 L processes and one 250 L process. These trends are shown in Figure 4.8.

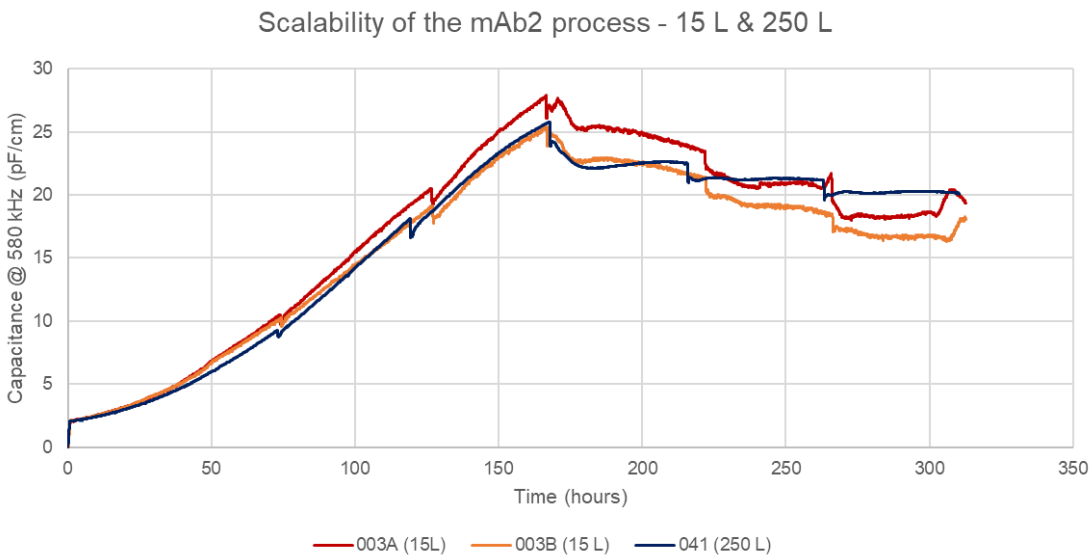

Figure 4.8 – Capacitance trends for all mAb2 processes at 15 L (red and orange) and 250 L (blue).

As with mAb1, the trends from 15 L and 250 L batches are highly similar. Again, this similarity is most prominent during the exponential growth phase, with more variation between batches during later stages of cultivation. The two 15 L batches follow a similar trend throughout the entire process (the difference in capacitance readings can be explained by higher offline VCD in mAb2-003A as compared to mAb2-003B), while the 250 L process has a slightly slower decrease in capacitance after the end of the exponential growth phase. It would be ideal to have data from more batches in order to further assess the similarity of the trends across scales, especially during the stationary and death phases, but this limited data does suggest that the mAb2 process is scalable.

4.1.5 Golden batch trajectories for mAb1 and mAb2

A golden batch trajectory is a highly beneficial tool, allowing early identification of issues by comparing the current trajectory to an established fingerprint based on previous successful batches. This can be used as an alarm system, which gets activated as soon as the capacitance deviates from the golden batch trajectory. Three successful batches of mAb1 were used to generate a golden batch trajectory for capacitance, shown in Figure 4.9. Similar golden batch trajectories were developed by Metze, Blioch et al. (2020), where the in-line capacitance measurements were able to detect deviations in cell growth trajectories earlier than offline cell counts.

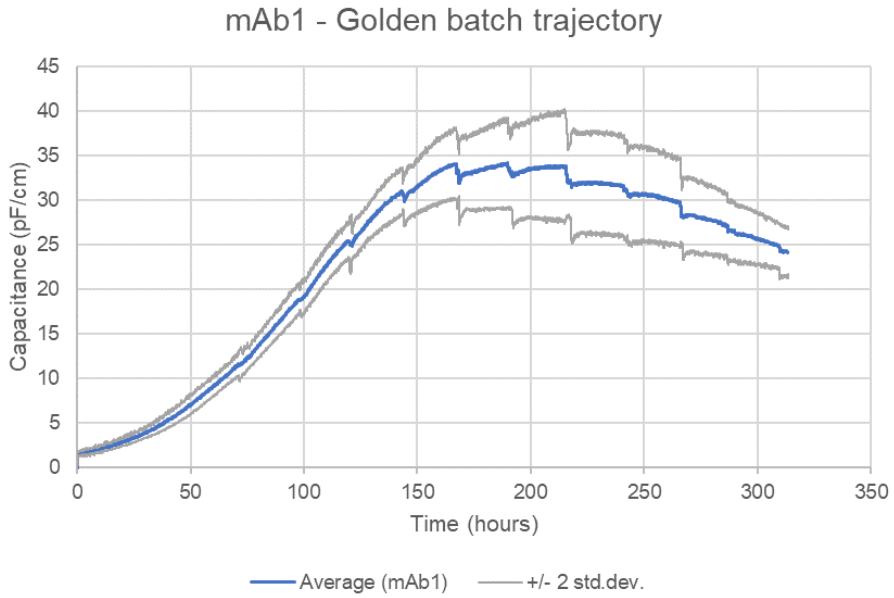

Figure 4.9 – Golden batch trajectory for mAb1. Upper and lower limits (2 SDs) are shown in grey.

Upper and lower limits were calculated by adding and subtracting two standard deviations from the average values. The use of this fingerprint is especially valuable in the exponential growth phase, as that is when capacitance gives the most accurate predictions of VCD. As seen in the golden batch trajectory for mAb1, the acceptable range for capacitance measurements formed by the upper and lower limits is quite narrow during the exponential growth phase. This means that any deviation from this trajectory would be detected quickly, allowing corrective actions to be taken to potentially recover the process. However, a potential limitation is any interference to the probe's measurements, such as the dip observed in capacitance in mAb1-025 (Figure 4.5). When using an automated alarm system connected to the capacitance trajectory, the first steps following the activation of the alarm would

involve ensuring that the deviation is not caused by an interference to the probe. This includes performing a "clean pulse" of the probe, which should remove any bubbles, as well as checking connections between the probe itself and the Futura.

A golden batch trajectory was also generated for mAb2, shown in Figure 4.10. This fingerprint was generated using only three batches of mAb2 with available capacitance data. As more capacitance data is gathered for this process, the fingerprint can be modified based on the most representative batches.

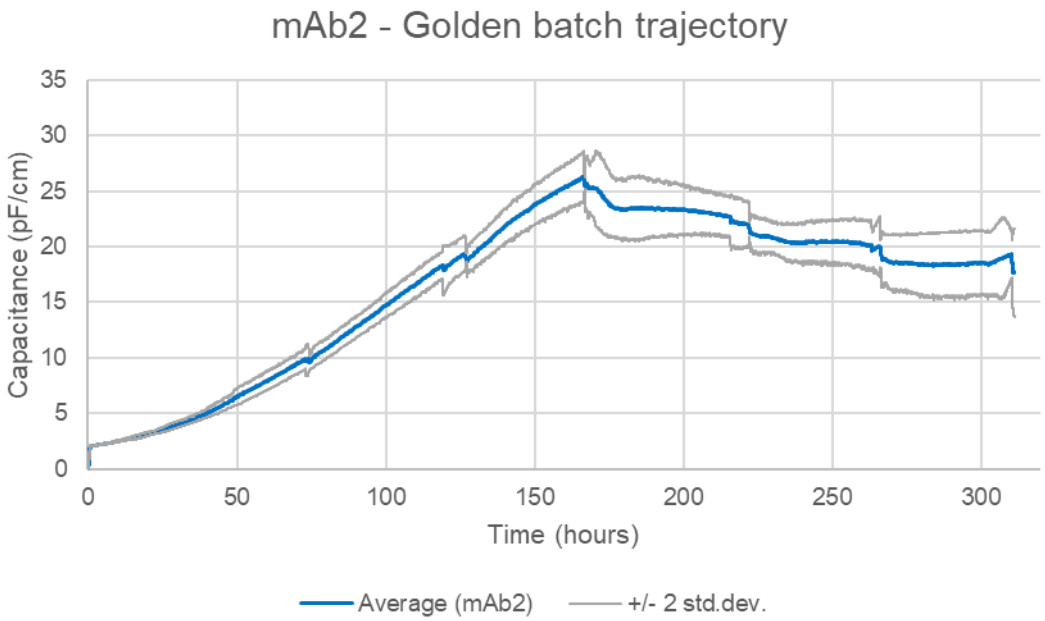

Figure 4.10 – Golden batch trajectory for mAb2. Upper and lower limits are shown in grey.

4.2 Correlation between capacitance and offline VCD

Linear modeling was used in the correlation of capacitance measurements with offline VCD measurements, as it is simple and a well established method in the calibration of capacitance for VCD predictions (Dabros et al., 2009). Figure 4.11 shows linear regression models for the correlation between capacitance and offline VCD in a mAb1 batch, for the entire process (Figure 4.11 a) and the exponential growth phase (Figure 4.11 b). The correlation is strong during the exponential growth phase, but less accurate when datapoints from the whole process are included. In the exponential growth phase, the R^2 is close to 1, whereas the data points are more widely distributed during the death phase, resulting in a lower coefficient of

determination (R^2 = 0.9617). This was expected, as the changes in cell diameter observed after the end of the exponential growth phase affect capacitance measurements, resulting in a wider distribution of data points. Compared to the exponential growth phase, each cell now contributes more to the readings, reducing the correlation between capacitance and VCD. Similar results were obtained for all the batches. This is illustrated in Figure 4.12, which shows an overview of R^2 values for capacitance/VCD correlation from all batches.

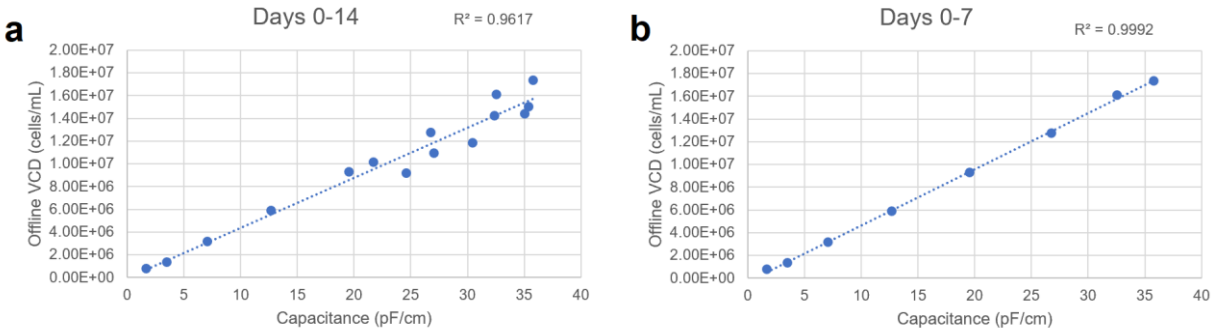

Figure 4.11 – Linear regression models for correlation between capacitance and offline VCD. (a) Values from the entire process. (b) Values from the exponential growth phase.

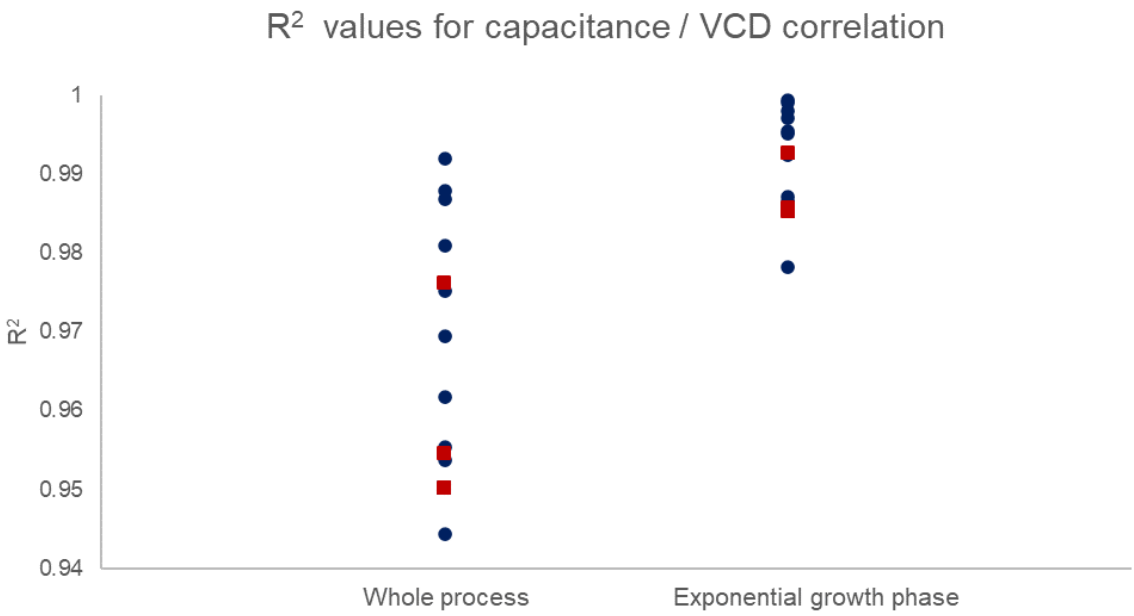

Figure 4.12 – R^2 values for capacitance/VCD correlation for all batches, for the whole process (left) and the exponential growth phase (right). Values from mAb1 batches are shown with blue circles and values from mAb2 batches are shown with red squares.

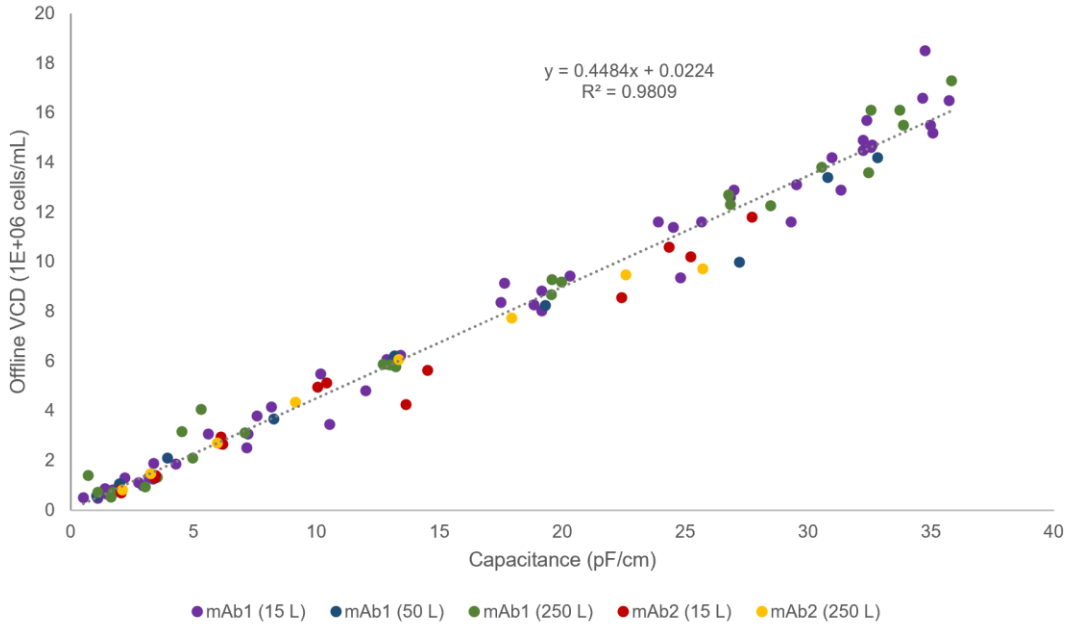

Figure 4.13 - Linear regression model of capacitance and offline VCD measurements for all batches of mAb1 and mAb2 across all scales.

Figure 4.13 shows a linear regression model that includes all batches of both mAb1 and mAb2 across all scales, using values from the exponential growth phase. The coefficient of determination is 98.09%. A high coefficient of determination indicates that the capacitance probe is able to predict the VCD in a highly accurate manner during this stage, and the scalability of this linear model shows that capacitance can be used as an in-line monitoring tool during process scale-up. As VCD is a key process parameter in biopharmaceutical production, directly related to the amount of product produced, it is important to establish consistency of cell growth trajectories when scaling up the process.

4.3 Biomass factor optimization

The biomass factor is a constant that is used to convert the measured capacitance signal (pF/cm) to VCD (cells/mL), calculated by dividing offline VCD with the measured capacitance. When developing a new process, a general biomass factor for that specific process can be generated and used to convert capacitance readings to VCD predictions in real-time in following batches.

The biomass factor for each process was calculated by dividing each datapoint for offline VCD with the corresponding capacitance reading, and then finding the average value of the biomass factor over the course of the whole run. The average biomass factor for the exponential growth phase was also calculated (days 0 to 7 or 8, depending on the batch). These biomass factors are shown in Table 4.1. mAb1-032A and mAb1-002A were excluded as they were terminated before day 8. mAb1-027A was contaminated on day 8, so the average biomass factor based on the whole run was not calculated.

Table 4.1- Biomass factors from all bioreactor runs.

Batch ID	**Scale**	**Biomass factor based on entire process**	**Biomass factor based on exponential growth phase**
mAb1-024	15 L	4.52E+05	4.51E+05
mAb1-027A	15 L	N/A	4.36E+05
mAb1-027B	15 L	4.61E+05	4.99 E+05
mAb1-032B	15 L	4.16 E+05	4.45 E+05
mAb1-001A	15 L	4.90 E+05	5.13 E+05
mAb1-001B	15 L	3.90 E+05	3.96 E+05
mAb1-002B	15 L	4.46 E+05	4.50 E+05
mAb2-003A	15 L	4.42 E+05	4.26 E+05
mAb2-003B	15 L	4.29 E+05	4.14 E+05
mAb1-021	50 L	4.48 E+05	4.66 E+05
mAb1-025	250 L	4.26 E+05	4.49 E+05
mAb1-030	250 L	4.30 E+05	4.58 E+05
mAb1-036	250 L	4.35 E+05	4.53 E+05
mAb2-041	250 L	4.25E+05	4.25E+05
Average (all batches)		**4.37E+05**	**4.49E+05**
Average (mAb1)		**4.38E+05**	**4.56E+05**
Average (mAb2)		**4.32E+05**	**4.22E+05**

Figure 4.14 shows the biomass factors for all 15 L and 250 L batches for the whole process as well as the exponential growth phase. The biomass factors for the mAb1 and mAb2 processes are very similar. However, as each cell line differs, resulting in different capacitance trends, it should not be assumed that these biomass factors will be applicable to every process. Thus, it may be important to generate a process-specific biomass factor when a new product is developed.

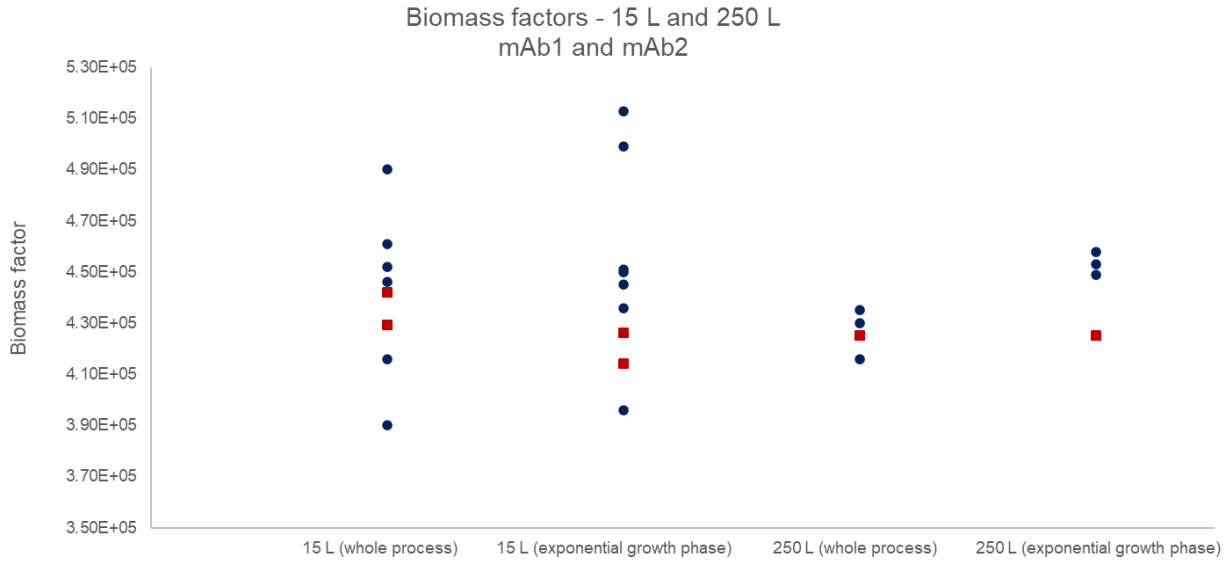

Figure 4.14 - Biomass factors for all batches of mAb1 and mAb2 at 15 L and 250 L scales. Biomass factors were calculated both based on the entire process and based on the exponential growth phase. Biomass factors from mAb1 batches are shown with blue circles and biomass factors from mAb2 batches are shown with red squares.

Since the correlation between capacitance and offline VCD is higher during the exponential growth phase, biomass factors calculated based on measurements from this part of the process will be used. As there was no significant difference between scales, a general biomass factor was calculated for each process using data from all scales. The average biomass factor for all mAb1 batches is 4.56E+05. However, there are several outliers (mAb1-027B, mAb1-001A and mAb1-001B). In order to generate a general biomass factor applicable for in-line monitoring of VCD, a biomass factor excluding these values was also calculated, resulting in a value of 4.51E+05. By applying this biomass factor to the capacitance readings in real-time, we should be provided with a relatively accurate prediction of VCD during the exponential growth phase. This is illustrated in Figure 4.15, where the general mAb1 biomass factor was applied to a batch with an unusually high batch-specific biomass factor (mAb1-027B, biomass factor 4.99E+05), resulting in an accurate VCD prediction for the majority of the process. As data from more batches is collected, the

biomass factor can simply be adjusted if needed. For mAb2, the average biomass factor based on the exponential growth phase is 4.22E+05, slightly lower than for mAb1. However, this is only based on data from three different batches. As more data is gathered, this biomass factor can be adjusted accordingly.

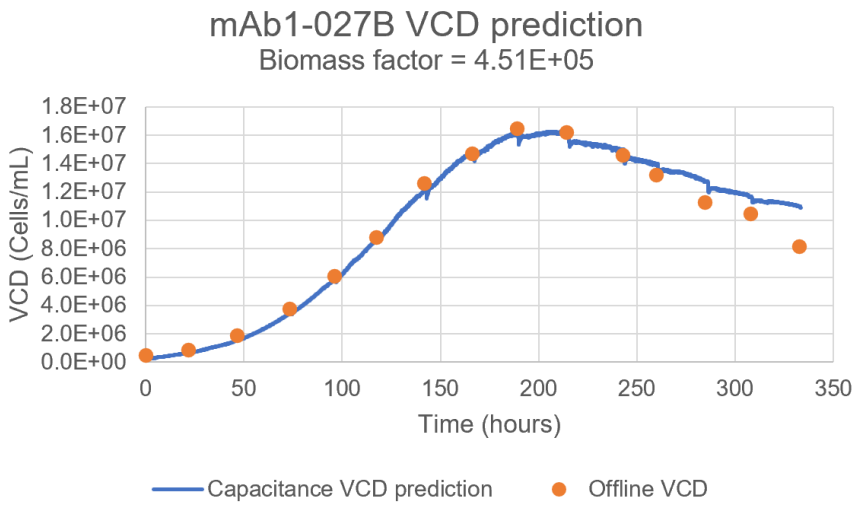

Figure 4.15 – VCD prediction for mAb1-027B using the general biomass factor developed for all mAb1 processes (4.51E+05).

4.4 Capacitance data vs questionable offline datapoints

Offline VCD measurements are often infrequent, e.g., once a day, whereas capacitance probes are able to take multiple measurements per minute. Figure 4.16 shows the capacitance-based VCD prediction from two batches that have several offline VCD data points that appear abnormal. In mAb1-002B (Figure 4.16 a), offline VCD on day 7 (and to a lesser extent day 8) is much higher than what is typically observed in other mAb1 batches. Here, the capacitance-based VCD prediction suggests that the VCD on day 7 is actually lower, around 1.56E+07 (offline measurement was 1.85E+07 cells/mL). In mAb2-041 (Figure 4.16 b), several offline VCD data points in the second half of the process are suspicious, with offline VCD measurements being inconsistent during this stage. While capacitance may not give accurate measurements of VCD during later stages of cultivation due to changes in cell size, this data does suggest that the offline measurements are inaccurate. Any offline analytics involves a risk of human error. Sampling is often performed

by different individuals, potentially resulting in differences in sampling techniques. Additionally, when measuring VCD at high cell densities, the culture needs to be manually diluted for each measurement, introducing additional opportunities for errors to occur. By receiving real-time feedback through capacitance measurements in combination with offline sampling results, we are better able to gauge the performance of the culture, rather than relying solely on infrequent offline data that may be inaccurate.

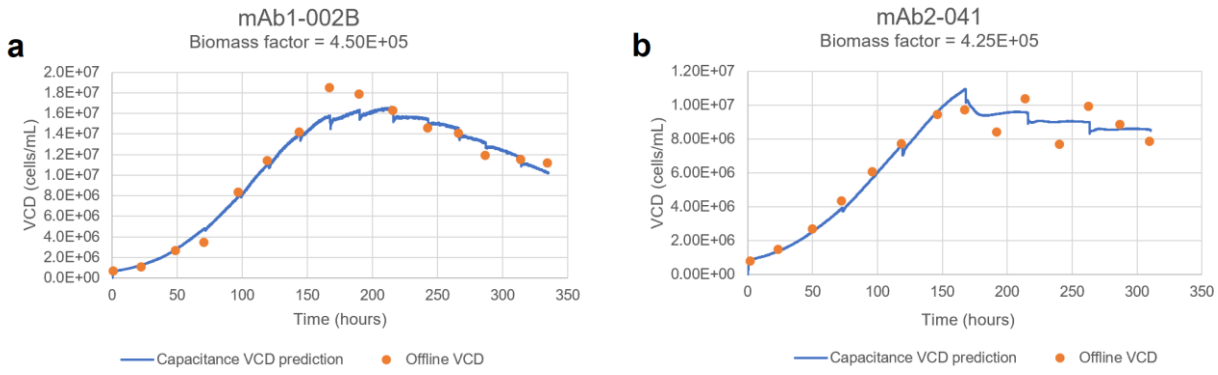

Figure 4.16 – Capacitance-based VCD prediction in two batches with offline measurements that appear abnormal. (a) mAb1-002B, which has unusually high offline VCD on day 7. (b) mAb2-041, where offline measurements are inconsistent during the second half of the cultivation.

4.5 Capacitance VCD predictions vs. Raman VCD predictions

Raman probes were included in several of the 15 L batches, allowing comparisons of these different VCD prediction methods. Figure 4.17 compares VCD prediction based on capacitance measurements to VCD predictions based on Raman spectroscopy for mAb1-001A. Capacitance and Raman VCD predictions both followed the offline VCD trend closely. Results from the other 15 L batches were highly similar. Capacitance readings gave a more stable VCD prediction trend, whereas VCD predictions based on Raman spectroscopy were more noisy. One reason is that the Raman probe acquires spectra less frequently than capacitance measurements, with Raman spectra being averaged over 12 minutes for each data point, contrary to capacitance probes that take measurements every 30 seconds. This is especially evident when it comes to the drops in VCD due to dilution of the culture during daily feeding. Overall, capacitance and Raman spectroscopy gave similar results for VCD prediction. Recent work by Rafferty et al. (2020) has proposed the combined

use of both of these PAT tools to support a feeding strategy based on in-line capacitance measurements.

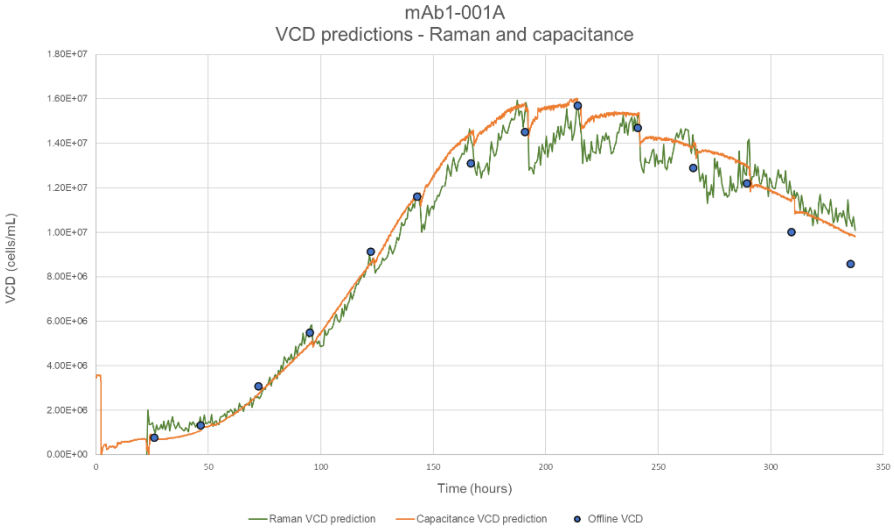

Figure 4.17 VCD predictions based on capacitance measurements (orange line) and Raman spectroscopy (green line). Offline VCD data is shown with blue circles.

4.6 Detection of bacterial contamination by conductivity

Bacterial contamination is a common issue in upstream processing. For example, contamination can occur if any of the materials used, such as bioreactor, tubing, media, feed, or the starting cell culture are not sterile. Any direct interaction with the culture, such as sample removal for analysis, also introduces contamination risks. To minimize the risk of contamination, every component going into the reactor must be sterile, the bioreactor needs to be sterilized prior to inoculation, and proper sampling techniques must be practiced.

Batch mAb1-027A was terminated early due to bacterial contamination. Here, a drop in capacitance occurred at 191 hours into the process. However, a sharp increase in conductivity began several hours before, at 185 hours, similar to the conductivity spike observed my Morris et al. (2021) upon bacterial contamination. Capacitance trends and conductivity trends from mAb1-027A (contaminated on day 8) and mAb1-027B (not contaminated) are shown in Figure 4.18. As conductivity generally rises slowly during the process, any sudden conductivity spikes may indicate that there is an issue, such as bacterial contamination.

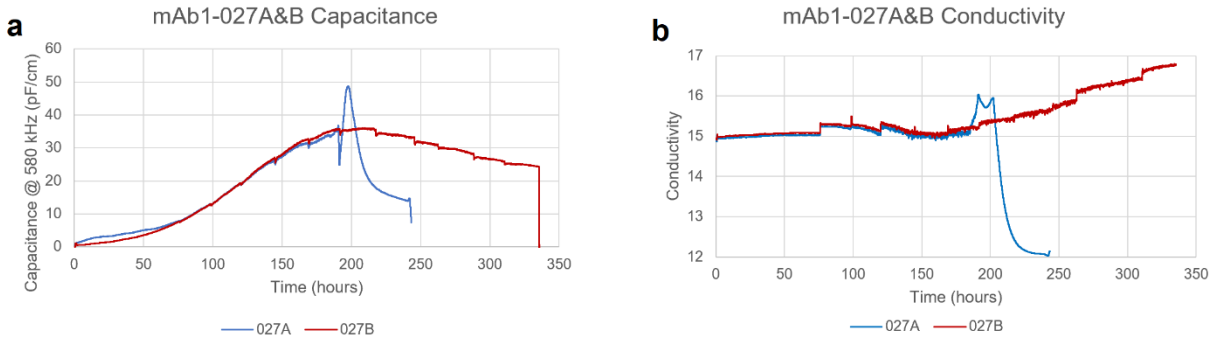

Figure 4.18 – (a) Capacitance trends for mAb1-027A (blue) and mAb1-027B (red). (b) Conductivity trends for mAb1-027A (blue) and mAb1-027B (red).

In mAb1-002A, there was an issue with the agitator where the impeller was not rotating. This resulted in a significant decrease in capacitance, as well as fluctuations in DO concentration. The cause of the abnormal capacitance and DO measurements was not detected until the following day. There was, however, no sharp increase in conductivity, which could have served as an indicator that the decrease in capacitance was not due to contamination. The capacitance and conductivity trends for mAb1-002A is shown in Figure 4.19.

The conductivity data gathered by capacitance probes can thus give us additional insight into the culture conditions, including detection of early signs of bacterial contamination – this would allow for contaminated batches to be terminated earlier, saving time and resources.

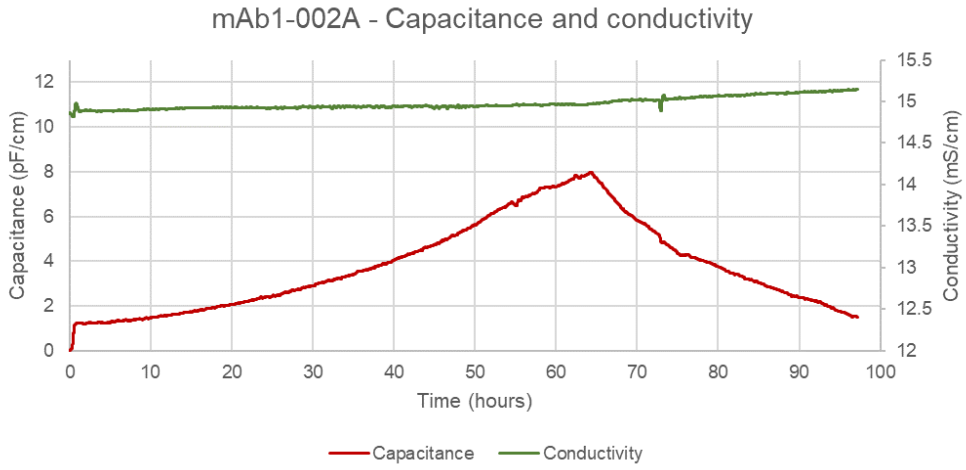

Figure 4.19 – Capacitance (red) and conductivity (green) trends for mAb1-002A.

5 Conclusions

Over the last decades, capacitance measurements have been widely applied as real-time monitoring tools of viable cell density in mammalian cell culture processes. In this work, capacitance probes were utilized in two different bioprocesses, and shown to be a reliable tool for in-line monitoring of VCD during the exponential growth phase regardless of scale. With the current emphasis on process understanding and process control in biopharmaceutical production, having a reliable and robust method for in-line monitoring of important parameters is highly valuable. The batch fingerprints developed here can serve as guidelines for the following batches and can be further optimized as more data from these processes is collected. The upper and lower approved limits for capacitance provided by these fingerprints enable quick reactions to process deviations.

The general biomass factors developed for the mAb1 and mAb2 processes can be applied to the capacitance readings of future batches in order to provide real-time VCD measurements. While eliminating sampling and relying solely on in-line data for VCD is not yet feasible for these processes, in-line capacitance data can be highly useful in combination with the offline VCD measurements in order to gain a more detailed insight into the progress of the cultivation.

A limitation of using single-frequency capacitance data is that once the exponential growth phase ends, it no longer provides a reliable real-time prediction of VCD. The goal, however, is to have a reliable in-line monitoring of VCD throughout the entire process. As the probes used here are able to measure across multiple frequencies, future work may be able to use multifrequency data to allow real-time monitoring of VCD throughout the entire bioreactor stage. By applying Cole-Cole modeling to multifrequency measurements, additional information about the cell culture can be extracted, such as the cell diameter, which can be used to generate a more accurate VCD prediction during the later stages of the cultivation.

In addition, by integrating the capacitance measurements into the bioreactor software-driven control unit, an automated feeding strategy based on capacitance measurements can be employed. In fed-batch processes, feed addition can be added when capacitance drops to a certain value. This can also be useful in perfusion processes, where the VCD needs to be kept at a target set point. Depending on the capacitance measurements, the system can

automatically add feed after drops in capacitance or perform a cell bleed after increases in capacitance.

To conclude, capacitance probes allow us to accurately monitor cell growth in real-time. Using this information, it is possible to react to process deviations quickly, resulting in a lower number of failed batches. As continuous monitoring of important parameters results in increased process knowledge, these in-line monitoring tools can be used to increase process robustness. Finally, in-line capacitance measurements can be used in combination with advanced control strategies to allow optimization of feeding strategies, inoculation, and harvest time, as well as enabling automated feeds and cell bleeds.

References

Abu-Absi, N. R., Kenty, B. M., Cuellar, M. E., Borys, M. C., Sakhamuri, S., Strachan, D. J., Hausladen, M. C., & Li, Z. J. (2011). Real time monitoring of multiple parameters in mammalian cell culture bioreactors using an in-line Raman spectroscopy probe. *Biotechnology and Bioengineering*, *108*(5), 1215–1221. https://doi.org/10.1002/bit.23023

Ansorge, S., Esteban, G., & Schmid, G. (2009). Multifrequency permittivity measurements enable on-line monitoring of changes in intracellular conductivity due to nutrient limitations during batch cultivations of CHO cells. *Biotechnology Progress*, NA-NA. https://doi.org/10.1002/btpr.347

Ansorge, S., Esteban, G., & Schmid, G. (2010). On-line monitoring of responses to nutrient feed additions by multi-frequency permittivity measurements in fed-batch cultivations of CHO cells. *Cytotechnology*, *62*(2), 121–132. https://doi.org/10.1007/s10616-010-9267-z

Bergin, A., Carvell, J., & Butler, M. (2022). Applications of bio-capacitance to cell culture manufacturing. *Biotechnology Advances*, 108048. https://doi.org/10.1016/j.biotechadv.2022.108048

Birch, J. R., & Racher, A. J. (2006). Antibody production. *Advanced Drug Delivery Reviews*, *58*(5–6), 671–685. https://doi.org/10.1016/j.addr.2005.12.006

Blackstone, E. A., & Joseph, P. F. (2013). The Economics of Biosimilars. *American Health & Drug Benefits*, *6*(8), 469–478.

Brechmann, N. A., Eriksson, P.-O., Eriksson, K., Oscarsson, S., Buijs, J., Shokri, A., Hjälm, G., & Chotteau, V. (2019). Pilot-scale process for magnetic bead purification of antibodies directly from non-clarified CHO cell culture. *Biotechnology Progress*, *35*(3), e2775. https://doi.org/10.1002/btpr.2775

Butler, M., & Meneses-Acosta, A. (2012). Recent advances in technology supporting biopharmaceutical production from mammalian cells. *Applied Microbiology and Biotechnology*, *96*(4), 885–894. https://doi.org/10.1007/s00253-012-4451-z

Camacho, W., & Karlsson, S. (2001). NIR, DSC, and FTIR as quantitative methods for compositional analysis of blends of polymers obtained from recycled mixed plastic waste. *Polymer Engineering & Science*, *41*(9), 1626–1635. https://doi.org/10.1002/pen.10860

Cannizaro, C., Gügerli, R., Marison, I., & von Stockar, U. (2003). On-line biomass monitoring of CHO perfusion culture with scanning dielectric spectroscopy. *Biotechnology and Bioengineering*, *84*(5), 597–610. https://doi.org/10.1002/bit.10809

Carvell, J. P., & Dowd, J. E. (2006). On-line Measurements and Control of Viable Cell Density in Cell Culture Manufacturing Processes using Radio-frequency Impedance. *Cytotechnology*, *50*(1–3), 35–48. https://doi.org/10.1007/s10616-005-3974-x

Challa, S., & Potumarthi, R. (2013). Chemometrics-Based Process Analytical Technology (PAT) Tools: Applications and Adaptation in Pharmaceutical and Biopharmaceutical Industries. *Applied Biochemistry and Biotechnology*, *169*(1), 66–76. https://doi.org/10.1007/s12010-012-9950-y

Chiu, M. L., Goulet, D. R., Teplyakov, A., & Gilliland, G. L. (2019). Antibody Structure and Function: The Basis for Engineering Therapeutics. *Antibodies*, *8*(4), 55. https://doi.org/10.3390/antib8040055

Claßen, J., Aupert, F., Reardon, K. F., Solle, D., & Scheper, T. (2017). Spectroscopic sensors for in-line bioprocess monitoring in research and pharmaceutical industrial application. *Analytical and Bioanalytical Chemistry*, *409*(3), 651–666. https://doi.org/10.1007/s00216-016-0068-x

Dabros, M., Dennewald, D., Currie, D. J., Lee, M. H., Todd, R. W., Marison, I. W., & von Stockar, U. (2009). Cole–Cole, linear and multivariate modeling of capacitance data for on-line monitoring of biomass. *Bioprocess and Biosystems Engineering*, *32*(2), 161–173. https://doi.org/10.1007/s00449-008-0234-4

Dumont, J., Euwart, D., Mei, B., Estes, S., & Kshirsagar, R. (2016). Human cell lines for biopharmaceutical manufacturing: history, status, and future perspectives. *Critical Reviews in Biotechnology*, *36*(6), 1110–1122. https://doi.org/10.3109/07388551.2015.1084266

European Medicines Agency. (2014, October 29). *Guideline on similar biological medicinal products*. Https://Www.Ema.Europa.Eu/En/Documents/Scientific-Guideline/Guideline-Similar-Biological-Medicinal-Products-Rev1_en.Pdf.

European Medicines Agency. (2019, October 19). *Biosimilars in the EU - Information guide for healthcare professionals*. Https://Www.Ema.Europa.Eu/En/Documents/Leaflet/Biosimilars-Eu-Information-Guide-Healthcare-Professionals_en.Pdf.

European Medicines Agency. (2022a, May 12). *Inflectra : EPAR - Product Information*. Https://Www.Ema.Europa.Eu/En/Documents/Product-Information/Inflectra-Epar-Product-Information_en.Pdf.

European Medicines Agency. (2022b, November 25). *Remisma : EPAR - Product Information*. Https://Www.Ema.Europa.Eu/En/Documents/Product-Information/Remsima-Epar-Product-Information_en.Pdf.

European Medicines Agency. (2022c, December 13). *European public assessment reports*. Https://Www.Ema.Europa.Eu/En/Medicines/Download-Medicine-Data.

Fischer, S., Handrick, R., & Otte, K. (2015). The art of CHO cell engineering: A comprehensive retrospect and future perspectives. *Biotechnology Advances*, *33*(8), 1878–1896. https://doi.org/10.1016/j.biotechadv.2015.10.015

Hamilton, R. G. (1987). Human IgG subclass measurements in the clinical laboratory. *Clinical Chemistry*, *33*(10), 1707–1725. https://doi.org/10.1093/clinchem/33.10.1707

Heled, Y. (2012). Why Primary Patents Covering Biologics Should be Unenforceable Against Generic Applicants under the Biologics Price Competition and Innovation Act. *Annals of Health Law*, *21*, 211–222.

Irani, V., Guy, A. J., Andrew, D., Beeson, J. G., Ramsland, P. A., & Richards, J. S. (2015). Molecular properties of human IgG subclasses and their implications for designing therapeutic monoclonal antibodies against infectious diseases. *Molecular Immunology*, *67*(2), 171–182. https://doi.org/10.1016/j.molimm.2015.03.255

Ishii-Watabe, A., & Kuwabara, T. (2019). Biosimilarity assessment of biosimilar therapeutic monoclonal antibodies. *Drug Metabolism and Pharmacokinetics*, *34*(1), 64–70. https://doi.org/10.1016/j.dmpk.2018.11.004

Johansson, J., Claybourn, M., & Folestad, S. (2010). *Raman Spectroscopy: A Strategic Tool in the Process Analytical Technology Toolbox* (pp. 241–262). https://doi.org/10.1007/978-3-642-02649-2_10

Jossen, V., Eibl, R., & Eibl, D. (2019). Single-Use Bioreactors – An Overview. In *Single-Use Technology in Biopharmaceutical Manufacture* (pp. 37–52). Wiley. https://doi.org/10.1002/9781119477891.ch4

Jungbauer, A. (2013). Continuous downstream processing of biopharmaceuticals. *Trends in Biotechnology*, *31*(8), 479–492. https://doi.org/10.1016/j.tibtech.2013.05.011

Keating, G. M., & Perry, C. M. (2002). Infliximab. *BioDrugs*, *16*(2), 111–148. https://doi.org/10.2165/00063030-200216020-00005

Kesik-Brodacka, M. (2018). Progress in biopharmaceutical development. *Biotechnology and Applied Biochemistry*, *65*(3), 306–322. https://doi.org/10.1002/bab.1617

Kim, J. Y., Kim, Y.-G., & Lee, G. M. (2012). CHO cells in biotechnology for production of recombinant proteins: current state and further potential. *Applied Microbiology and Biotechnology*, *93*(3), 917–930. https://doi.org/10.1007/s00253-011-3758-5

Kindt, T. J., Osborne, B. A., & Goldsby, R. A. (2006). *Kuby Immunology* (Sixth Edition). W. H. Freeman & Company.

Kulbacka, J., Choromańska, A., Rossowska, J., Wężgowiec, J., Saczko, J., & Rols, M.-P. (2017). Cell Membrane Transport Mechanisms: Ion Channels and Electrical Properties of Cell Membranes. In J. Kulbacka & S. Satkauskas (Eds.), *Transport Across Natural and Modified Biological Membranes and its Implications in Physiology and Therapy* (pp. 39–58). https://doi.org/10.1007/978-3-319-56895-9_3

Lim, H. C., & Shin, H. S. (2013). *Fed-Batch Cultures: Principles and Applications of Semi-Batch Bioreactors*. Cambridge University Press.

Long, D. A. (1971). Raman Spectroscopy. In L. A. K. Staveley (Ed.), *The Characterization of Chemical Purity: Organic Compounds* (pp. 149–162). Butterworths Scientific Publications.

Lu, R.-M., Hwang, Y.-C., Liu, I.-J., Lee, C.-C., Tsai, H.-Z., Li, H.-J., & Wu, H.-C. (2020). Development of therapeutic antibodies for the treatment of diseases. *Journal of Biomedical Science*, *27*(1), 1. https://doi.org/10.1186/s12929-019-0592-z

Makurvet, F. D. (2021). Biologics vs. small molecules: Drug costs and patient access. *Medicine in Drug Discovery*, *9*, 100075. https://doi.org/10.1016/j.medidd.2020.100075

Mehra, S., Chandrawanshi, V., & Prashad, K. (2017). Advanced Bioprocess Engineering: Fed-Batch and Perfusion Processes. In *Applied Bioengineering* (pp. 417–468). Wiley-VCH Verlag GmbH & Co. KGaA. https://doi.org/10.1002/9783527800599.ch14

Metze, S., Blioch, S., Matuszczyk, J., Greller, G., Grimm, C., Scholz, J., & Hoehse, M. (2020). Multivariate data analysis of capacitance frequency scanning for online monitoring of viable cell concentrations in small-scale bioreactors. *Analytical and Bioanalytical Chemistry*, *412*(9), 2089–2102. https://doi.org/10.1007/s00216-019-02096-3

Metze, S., Ruhl, S., Greller, G., Grimm, C., & Scholz, J. (2020). Monitoring online biomass with a capacitance sensor during scale-up of industrially relevant CHO cell culture fed-batch processes in single-use bioreactors. *Bioprocess and Biosystems Engineering*, *43*(2), 193–205. https://doi.org/10.1007/s00449-019-02216-4

Microsoft Corporation. (2018). Microsoft Excel. Retrieved from https://office.microsoft.com/excel

Moorkens, E., Jonker-Exler, C., Huys, I., Declerck, P., Simoens, S., & Vulto, A. G. (2016). Overcoming Barriers to the Market Access of Biosimilars in the European Union: The Case of Biosimilar Monoclonal Antibodies. *Frontiers in Pharmacology*, *7*. https://doi.org/10.3389/fphar.2016.00193

Morris, C., Madhavarao, C. N., Yoon, S., & Ashraf, M. (2021). Single in-line biomass probe detects CHO cell growth by capacitance and bacterial contamination by conductivity in bioreactor. *Biotechnology Journal*, *16*(12), 2100126. https://doi.org/10.1002/biot.202100126

Nezlin, R. (1998). General Characteristics of Immunoglobulin Molecules. In *The Immunoglobulins* (pp. 3–73). Elsevier. https://doi.org/10.1016/B978-012517970-6/50001-1

Opel, C. F., Li, J., & Amanullah, A. (2010). Quantitative modeling of viable cell density, cell size, intracellular conductivity, and membrane capacitance in batch and fed-batch CHO processes using dielectric spectroscopy. *Biotechnology Progess*, *26*(4), 1187–1199. https://doi.org/10.1002/btpr.425

Pörtner, R. (2015). *Bioreactors for Mammalian Cells* (pp. 89–135). https://doi.org/10.1007/978-3-319-10320-4_4

Rafferty, C., O'Mahony, J., Rea, R., Burgoyne, B., Balss, K. M., Lyngberg, O., O'Mahony-Hartnett, C., Hill, D., & Schaefer, E. (2020). Raman spectroscopic based chemometric models to support a dynamic capacitance based cell culture feeding strategy.

Bioprocess and Biosystems Engineering 43, 1415-1429. https://doi.org/10.1007/s00449-020-02336-2

Rathore, A. S., Bhambure, R., & Ghare, V. (2010). Process analytical technology (PAT) for biopharmaceutical products. *Analytical and Bioanalytical Chemistry*, *398*(1), 137–154. https://doi.org/10.1007/s00216-010-3781-x

Rish, A. J., Drennen, J. K., & Anderson, C. A. (2022). Metabolic trends of Chinese hamster ovary cells in biopharmaceutical production under batch and fed-batch conditions. *Biotechnology Progress*, *38*(1). https://doi.org/10.1002/btpr.3220

Rogge, P., Müller, D., & Schmidt, S. R. (2015). The Single-Use or Stainless Steel Decision Process: A CDMO Perspective . *BioProcess International*, *13*(11s).

Schiestl, M., Zabransky, M., & Sörgel, F. (2017). Ten years of biosimilars in Europe: development and evolution of the regulatory pathways. *Drug Design, Development and Therapy*, *Volume 11*, 1509–1515. https://doi.org/10.2147/DDDT.S130318

Shukla, A. A., & Gottschalk, U. (2013). Single-use disposable technologies for biopharmaceutical manufacturing. *Trends in Biotechnology*, *31*(3), 147–154. https://doi.org/10.1016/j.tibtech.2012.10.004

Shukla, A. A., Hubbard, B., Tressel, T., Guhan, S., & Low, D. (2007). Downstream processing of monoclonal antibodies—Application of platform approaches. *Journal of Chromatography B*, *848*(1), 28–39. https://doi.org/10.1016/j.jchromb.2006.09.026

Shuptrine, C. W., Surana, R., & Weiner, L. M. (2012). Monoclonal antibodies for the treatment of cancer. *Seminars in Cancer Biology*, *22*(1), 3–13. https://doi.org/10.1016/j.semcancer.2011.12.009

Smith, M. T., Madsen, B., Hsiao, T. B., & Jones, N. (2018, August 15). *Single-Use Bioreactors: Performance and Usability Considerations, Part 2*. Https://Bioprocessintl.Com/Upstream-Processing/Bioreactors/Single-Use-Bioreactors-Performance-and-Usability-Considerations-Part-2/.

Steinwedel, T., Dahlmann, K., Solle, D., Scheper, T., Reardon, K. F., & Lammers, F. (2019). Sensors for Disposable Bioreactor Systems. In *Single-Use Technology in Biopharmaceutical Manufacture* (pp. 69–82). Wiley. https://doi.org/10.1002/9781119477891.ch6

Streefland, M., Martens, D. E., Beuvery, E. C., & Wijffels, R. H. (2013). Process analytical technology (PAT) tools for the cultivation step in biopharmaceutical production. *Engineering in Life Sciences*, *13*(3), 212–223. https://doi.org/10.1002/elsc.201200025

Subramanian, A., & Rodriguez-Saona, L. (2009). Fourier Transform Infrared (FTIR) Spectroscopy. In D.-W. Sun (Ed.), *Infrared Spectroscopy for Food Quality Analysis and Control* (pp. 145–178). Elsevier. https://doi.org/10.1016/B978-0-12-374136-3.X0001-6

Tang, Y., Cain, P., Anguiano, V., Shih, J. J., Chai, Q., & Feng, Y. (2021). Impact of IgG subclass on molecular properties of monoclonal antibodies. *MAbs*, *13*(1). https://doi.org/10.1080/19420862.2021.1993768

Thermo Fisher Scientific. (2021). *HyPerforma DynaDrive Single-Use Bioreactor*. http://assets.thermofisher.com/TFS-Assets/BPD/Datasheets/3000-and-5000l-dynadrive-sub-data-sheet.pdf

Thomson, C. A. (2016). IgG Structure and Function. In *Encyclopedia of Immunobiology* (pp. 15–22). Elsevier. https://doi.org/10.1016/B978-0-12-374279-7.05002-5

U.S. Food and Drug Administration. (2022, December 19). *Biosimilar Product Information.* https://www.fda.gov/drugs/biosimilars/biosimilar-product-information

Vulto, A. G., & Jaquez, O. A. (2017). The process defines the product: what really matters in biosimilar design and production? *Rheumatology*, *56*(suppl_4), iv14–iv29. https://doi.org/10.1093/rheumatology/kex278

Yu, J., Song, Y., & Tian, W. (2020). How to select IgG subclasses in developing anti-tumor therapeutic antibodies. *Journal of Hematology & Oncology*, *13*(1), 45. https://doi.org/10.1186/s13045-020-00876-4

Zahavi, D., & Weiner, L. (2020). Monoclonal Antibodies in Cancer Therapy. *Antibodies*, *9*(3), 34. https://doi.org/10.3390/antib9030034